2023

Nanomaterials-Based Biosensors for the Detection of Prostate Cancer Biomarkers: Recent Trends and Future Perspective

Baljit Singh
Technological University Dublin, Ireland, baljit.singh@tudublin.ie

Shiliang Ma
Technological University Dublin, Ireland, shiliang.ma@tudublin.ie

Tony O. Hara
Department of Agriculture, Food and the Marine, Backweston Laboratory Campus, Celbridge, County Kildare, W23 X3PH Ireland

See next page for additional authors

Recommended Citation

Authors

Baljit Singh, Shiliang Ma, Tony O. Hara, and Sargun Singh

Nanomaterials-Based Biosensors for the Detection of Prostate Cancer Biomarkers: Recent Trends and Future Perspective

Baljit Singh,* Shiliang Ma, Tony O. Hara, and Sargun Singh

Cancer is among the leading causes of death and an important barrier to improving life expectancy globally. Prostate cancer is the second most common cancer in men worldwide. The detection of biomarkers in body fluids is the key topic for the diagnosis and prognosis of prostate cancer. Despite advances in prostate cancer detection methods, therapeutic agents and new biomarkers, prostate cancer remains a serious challenge. Prostate-specific antigen (PSA) is widely recognized as an important biomarker for the diagnosis of prostate cancer although researchers have also investigated the use of alternative biomarkers. Design and development of novel biosensors for prostate cancer detection has become a hot research area with advances in nanotechnology aiding biosensor development. This article reviews recent achievements and progress that nanomaterials and nanotechnology have made in biomarkers based biosensors for prostate cancer detection and covers: i) PSA-targeted biosensors (immunosensors, aptamer-based, peptide-based and nanopore-based biosensors), ii) sarcosine oxidase-targeted biosensors, iii) other biomarkers based biosensors (prostate cancer antigen 3 (PCA3), vascular endothelial growth factor (VEGF) and prostate-specific membrane antigen (PSMA)) including dual biomarkers based biosensors (PSA-VEGF, PSA-PSMA, PSA-PCA3 and PSA-sarcosine). The aim of this review is to provide insights into how nanomaterials in combination with various biomarkers are now aiding biosensor development in prostate cancer diagnostics.

1. Introduction

Cancer ranks as a leading cause of death as well as an important barrier to improved life expectancy globally.[1] Cancer is the first or second leading cause of death in people under the age of 70 in 112 out of 183 countries and ranks third or fourth in a further 23 countries, as per the estimates from the World Health Organization (WHO, 2019).[2] Prostate cancer is the second most common cancer in men worldwide.[3] Although early diagnosis can effectively improve patients' quality of life and prolong survival time, current diagnostic methods still lack the sensitivity, accuracy, and specificity for clinical diagnostic applications.[4] Therefore, it is necessary to find improved diagnostic tools with high selectivity, sensitivity, and stability. With developments in the healthcare field, biosensors present a new type of solution, which have advantages such as lower design and production costs, high sensitivity and specificity, and portability.[5] There are a wide variety of prostate cancer biomarkers such as

B. Singh, S. Ma
MiCRA Biodiagnostics Technology Gateway
Technological University Dublin (TU Dublin)
Dublin 24 D24 FKT9, Ireland
E-mail: baljit.singh@tudublin.ie
B. Singh
Centre of Applied Science for Health
Technological University Dublin (TU Dublin)
Dublin 24 D24 FKT9, Ireland

T. O. Hara
Pesticide Registration Division
Department of Agriculture, Food and the Marine
Backweston Laboratory Campus, Celbridge
County Kildare W23 X3PH, Ireland
S. Singh
Old Bawn Community School
Old Bawn
Tallaght, Dublin 24 D24 HP38, Ireland

**ADVANCED
SCIENCE NEWS**

www.advancedsciencenews.com

**ADVANCED
MATERIALS
TECHNOLOGIES**

www.advmattechnol.de

Table 1. Biomarkers (reviewed in this review) along with their testing methods.

Biomarker	Testing methods including gold-standard
PSA	PSA-test/DRE/MRI/Biopsy
Sarcosine	ELISA/HPLC-MS/Biopsy
PCA3	PCA3-test/Transcription-mediated amplification (TMA)/DRE/MRI/Biopsy
VEGF	ELISA/Biopsy
PSMA	PSMA positron emission tomography (PET)/computed tomography (CT)/ELISA/IHC/MRI/Biopsy

PSA, PCA3, sarcosine oxidase and so on. PSA is amongst the most common biomarkers used in prostate cancer diagnosis. When its concentration in the blood is greater than 4 ng mL^{-1}, it is considered an indicator of early stage of prostate cancer. At greater than 10 ng mL^{-1}, it can be considered a clear indicator of disease onset. However, test results can be controversial when PSA is the only screening biomarker.[6] In past 20 years, main limitation of PSA-based detection was lack of specificity wherein the biopsy reports corroborated negative result in more than 75% men even with the PSA level in the range of 4.0–10.0 ng mL^{-1}.[6] On the other hand, the usual PSA test needs to be carried out in a dedicated biochemical laboratory, and it needs to be analysed using large, automated analysers and equipment. This requires transport and storage of samples, which in turn require long waiting times and increased costs. In addition to PSA, other biomarkers are also considered in this review and are summarized below (**Table 1**).

Biosensors are functionally composed of three components. The biological recognition element, responsible for detecting the analyte and generating a response signal, forms the first part of the biosensor. The signal generated by the biological recognition element is then transformed into a detectable response by the second component called a transducer. The third part of the biosensor is the detector that amplifies and processes the signal before displaying it using an electronic display system.[7,8] Biosensors are designed as a self-contained analytical device that typically converts chemical or physical signals into electrical signals. PSA-targeted biosensors are mainly immunosensors, which are based on specific antibody-antigen interactions to form stable immune complexes that present an altered electrical signal in electrochemical analysis. In addition to specific antibody-antigen interactions, aptamer-based biosensors for biomedical diagnostics are also reported.[9] Aptamers are single-stranded nucleic acids that selectively bind to target molecules. Most aptamers are obtained through a combinatorial biology technique (SELEX). Peptides interactions have also been used as components in biosensors fabrication and biological analysis due to various reasons including mature synthesis protocols, diverse structures, and selective substrates for enzymes. Bio-conjugation strategies can provide an efficient way to convert the interaction between peptides and analytes into a measurable signal.[10]

Various nanomaterials and nanocomposites for biosensing applications are reported.[11] The development of nanomaterials and their use as transducers are making advancements in the biosensing applications and cancer detection.[5,12] In recent years, as more and more biosensors have been developed, we can see

that nanomaterials offer a variety of advantages, for example, electrodes modified with graphene family nanocomplexes can improve signal transmission.[11] Titanium (Ti) family nanocomposites are advantageous in facilitating the redox reactions. TiO_2 material showed potential in biosensing with advantages such as high bio-inertness and resistance to corrosion from the bodily fluids.[12] A combined effort of having a reliable biomarker for cancer detection and a sophisticated and compact detection system, e.g. TiO_2-based nanobiosensor, could facilitate the cancer biomarkers detection and diagnostics development.[12] In addition to these, there are many nanocomposites of transition metals that are cost-effective and more environmentally friendly. However, conventional biosensors for single biomarkers inevitably encounter the problem of false positive test results caused by non-specific recognition and environmental interference.[11,13] To overcome the limitations of prostate cancer biosensors based on single biomarker, next generation and multiple biomarkers will be required for cancer detection, as this increases diagnostic sensitivity, specificity and accuracy.[14] Pan et al. introduced VEGF, another cancer biomarker and developed a graphene oxide/ssDNA (GO-ssDNA) based system that can measure VEGF and PSA simultaneously.[15] This dual examination approach may offer a more accurate and faster alternative to current tests.

Dual-mode biosensors are an important topic of research at this stage. However, the development of prostate cancer-based biosensors is still in its infancy and there are three main challenges 1) assay sensitivity, 2) response time, and 3) selectivity that need to be addressed.[16] To date, there is still no prostate cancer-based biosensor that can overcome all these problems. Most of the biosensor development is still in the laboratory stage and there is a long way to go for its commercialization. The introduction of the Point of Care (POC) concept requires diagnostic testing to be performed outside of the clinical laboratory and near where the patient is receiving care. POC biosensors should meet the requirements of high precision, promptness in detection, reproducibility, ease of use and reduce the need for complicated instrumentation and high levels of technical skills amongst users. Therefore, exploring new biomarkers and matching biosensor materials has become one of the mainstreams of developing prostate cancer biosensors. This review summarizes recent advances in nanomaterials and approaches employed in biosensors for prostate cancer detection (**Figure 1**). The discussions below focus on the use of nanomaterials to construct specific biomarker biosensors based on selected articles published in the past few years. We hope that this review will bring increased awareness of the potential benefits that biosensors have to offer in prostate cancer diagnostics and the role that nanomaterials are playing in their development.

2. PSA-Targeted Biosensors

A common target in prostate cancer biomarkers development is the desire of non-invasive assays to replace "biopsy" as the diagnostic "gold standard".[14] PSA, also known as Human kallikrein 3 (hK3 or KLK3), is a product specific to prostate epithelial cells .[17] PSA is one of the few biomarkers routinely used for detection, risk stratification and monitoring of a common cancer.[18] Studies in the field of PSA detection and diagnosis have emerged in the late 20th century and the major trend during that period is
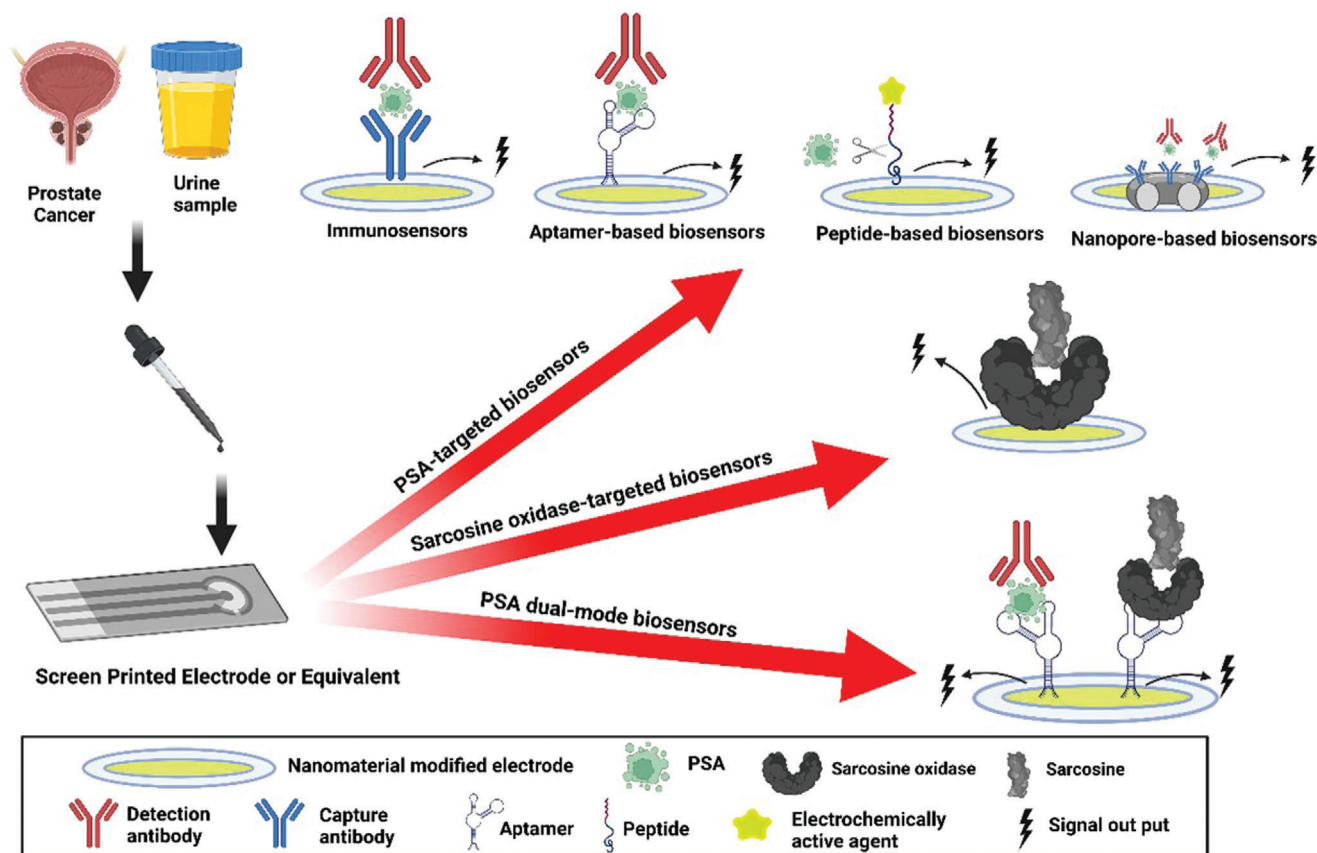
**ADVANCED
SCIENCE NEWS**

www.advancedsciencenews.com

**ADVANCED
MATERIALS
TECHNOLOGIES**

www.advmattechnol.de

Figure 1. Schematic illustration of nanomaterials-based biosensors and approaches for the detection of prostate cancer biomarkers.

utilization of automated high-throughput systems (to test multiple samples simultaneously to save the time of the staff). Unfortunately, large-scale detection systems increase the time of testing and lead to delays in diagnosis.[19] However, with advantages such as high sensitivity, low cost and rapid detection, attention has increasingly focused on the development of biosensor for prostate cancer detection. When it comes to biosensors for detecting PSA in blood, several approaches have been employed so far. In addition to nanopore-based biosensors, and depending on the biometric element type, biosensors for PSA detection can be classified into biosensors based on antibody (immunosensors), aptamer (aptasensors), and peptide (peptisensors).[5]

2.1. Immunosensors

Immunosensors are based on specific antibody-antigen interactions that form stable immune complexes. Antigen-specific detection antibodies (i.e., biometric recognition elements) are usually immobilized on the surface of nanomaterials, and they interact with biomarkers or antigens to produce physicochemical reactions that modulate signal readout. To preserve the biological activity of the antibody, prolonging the biosensors lifetime, and providing reusable and higher control over the orientation of the antibodies for higher detection capabilities, covalent bonding methods (e.g., EDC/NHS method (N-ethyl-N′-(3-(dimethylamino)propyl)carbodiimide/*N*-

hydroxysuccinimide) are widely used to immobilize recognition elements on the surface of nanoparticles (NPs).[20] In addition, graphene oxide (GO) has also been used in recent years to develop electrochemical devices thanks to its large surface area, 2D structure, low cost, production scalability, easy processing, and good compatibility.[21] Based on a case study of electrochemical synthesis of gold (Au)NP graphene composites, Pal et al.[21] points out that graphene-based biosensors made by electrochemical process may provide many potential applications for the detection of different cancer biomarkers; in particular, PSA in clinical settings. Drawing on insights from immobilization of monoclonal anti-PSA antibody via EDC/NHS coupling method, the authors have mapped out a low-cost, high-sensitivity electrochemical immunosensor to detect PSA (**Figure 2**). In his paper, the Au-GO biosensor was effectively applied to the detection of PSA in human serum samples with satisfactory results and limit of detection (LOD, 0.24 fg mL^{-1}).[21]

Slightly different from using Au-GO to immobilize anti-PSA antibodies, Farzin et al. did not adopt AuNPs, but directly functionalized GO by histidine (His-) and immobilized it on multiwalled carbon nanotubes (MWCNTs) (**Figure 3**).[22] The anti-PSA antibody was also immobilized by EDC/NHS covalent coupling method. Previous research has established that carbon nanotubes (CNTs) offer attractive opportunities for developing nanodevices and refining already existing analytical platforms, owing to their high mechanical power and electrical and thermal conductivity.[23] Farzin points out that the presence of anti-PSA
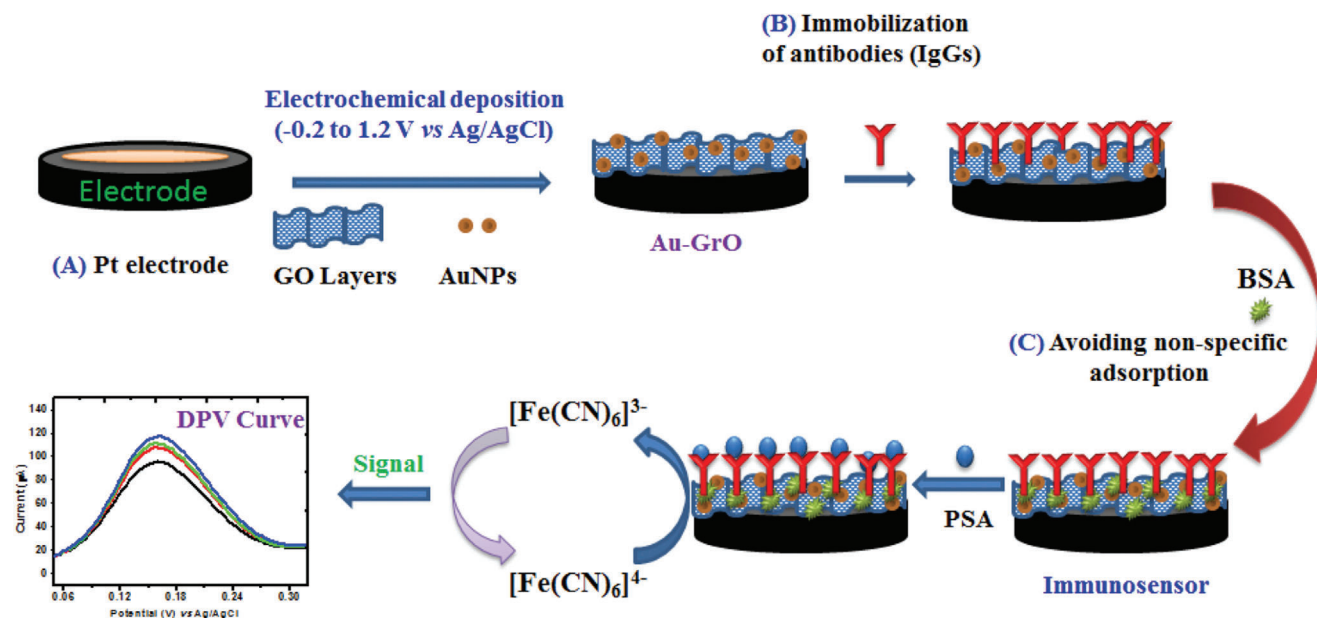
**ADVANCED
SCIENCE NEWS**

www.advancedsciencenews.com

**ADVANCED
MATERIALS
TECHNOLOGIES**

www.advmattechnol.de

Figure 2. Schematic illustration of the fabrication process for an electrochemical sensor (Au-GO) based on monoclonal anti-PSA antibody immobilized on AuGO electrode. Reproduced with permission.[21] Copyright 2017, Elsevier.

antibody blocked the electron transfer of thionine and decreased redox signals (detection limit = 2.8 fg mL^{-1} for PSA).[22] Her proposed immunosensor was able to selectively detect PSA because it was based on the selective interaction of PSA with thionine-NH$_2$-GO−COOH-Ab that led to a further decrease in the response current of the attached electrochemical probe. Generally, the MWCNT/His-rGO nanoplatform significantly amplifies the detection signal of PSA. It could be a useful hint for developing biomarkers with low signals, but it still has scope for improvement. As shown in **Table 2**, some recently reported PSA electrochemical immunosensing methods were compared with the MWCNT/His-rGO nanoplatform. It is evident that in addition to the GO-AuNPs platform, the MWCNT/His-rGO nanoplatform excels in terms of LOD. Therefore, it can be reasonably inferred that the nanocomplexes of the graphene family have a great advantage in terms of LOD.

The use of nanomaterials for signal amplification, increasing biomolecular loading capacity, and enhancing charge transfer has received extensive attention.[34] However, in addition to electrochemical sensors, there is considerable literature on localized surface plasmon resonance (LSPR) biosensors. LSPR is a phenomenon of collective oscillations by electrons in noble metal nanoparticles excited by external light.[35] LSPR based biosensing technology stands out among the optical sensors by virtue of its high sensitivity, direct, real-time and label-free detection capabilities.[36] In particular, the sensor fabricated with AuNPs can sensitively output a linear response according to the change in refractive index.[34,37] It is now well established from a variety of studies that nanomaterial based LSPR sensors generally exhibit good performance at low LOD values for the detection of cancer biomarkers in different media.[38] Additionally, Fattahi highlights that in the traditional structure of SPR sensors based on PSA detection, replacing optical fibers (FO) with a prism in the conventional structure of the SPR sensor can be a

novel tool for creating low-cost, remote sensing, miniaturized, and in vivo sensors (**Figure 4**).[38b] Kim is one of the pioneer scholars who applied fiber-optic localized surface plasmon resonance (FOLSPR) sensors for the PSA tests.[39] He found that sensors immersed in water require exposure to air while measuring, which can lead to drying of biomolecules and surface tension-induced rearrangement of nanoparticles. To minimize the resulting errors, FOLSPR sensor was combined with a microfluidic channel. Besides, to correct non-uniformity among the detected PSA results, a calibration method was adopted. In his influential examination, the microfluidic channel and calibration increased linearity and improved the sensitivity and dynamic range of PSA measurements.[40] In 2019, several improved processes for the FOLSPR biosensor were carried out by Kim et al. On the one hand, to overcome the lack of durability and fabrication reproducibility due to the rearrangement and size irregularity of metal nanoparticles, focused ion beam (FIB) milling technology was employed to construct nanodisk arrays. Using FIB milling for the nanostructure formation allows the precise control of the nanostructure size and shape, improving the reproducibility and durability of the sensor.[35] On the other hand, his research team also proposed a simple and low-cost physical method to immobilize AuNPs on optical fibers and developed a NP size regulation technology to achieve better adhesion of AuNPs to the surface. Finally, the FOLSPR sensor has a LOD of 124 fg mL^{-1} for PSA.[40] Much work on the potential of PSA based FOLSPR sensor has been carried out, however there are still some critical issues. Fattahi argues that the agglomeration of nanoparticles and cross-reactivity antibodies are major constraints on this technology.[38b] Meanwhile, another seminal study of PSA-based FOLSPR sensors by Kim et al. has attracted widespread attention. He designed a 3D nanostructure fabricated by growing the ZnO nanowires on the cross-section of optical fibers, and immobilizing AuNPs on the nanowires
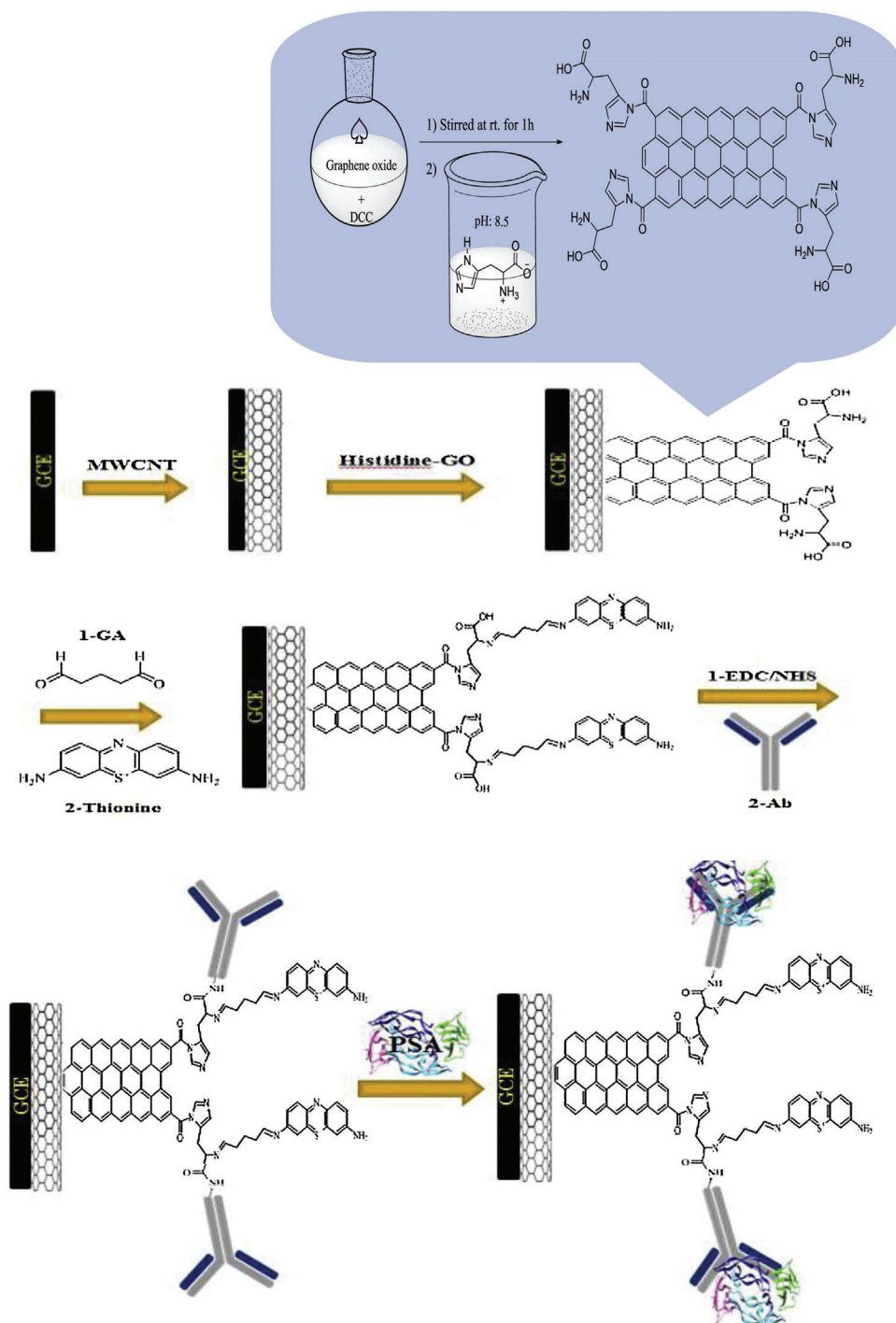
**ADVANCED
SCIENCE NEWS**

www.advancedsciencenews.com

**ADVANCED
MATERIALS
TECHNOLOGIES**

www.advmattechnol.de

Figure 3. Schematic illustration of the stepwise immunosensor fabrication process. Reproduced with permission.[22] Copyright 2019, Elsevier.

(**Figure 5**).[41] In addition, the LOD of the 3D nanostructure sensor was improved by 404% compared with the 2D nanostructure. This technology effectively improves the fiber space utilization of the FOLSPR sensor. However, this paper makes no attempt to specify whether the 3D nanostructure could solve the problem of agglomeration and cross-reactivity antibodies. Collectively, these studies outline a critical role for PSA based FOLSPR

sensor. Another interesting approach for PSA detection includes that reported by Rissin et al. who developed a Digital ELISA method (single-molecule enzyme-linked immunosorbent assay, which could detect as few as ≈10–20 enzyme-labeled complexes in 100 µL of sample (≈10^{-19} M) and allowed detection of clinically relevant proteins in serum at concentrations (<10^{-15} M). This approach detected PSA in sera from patients undergone

Table 2. Summary of selected nanomaterials based electrochemical immunosensors for prostate cancer (PSA biomarker) detection.

Type of nanomaterials	LOD	DLR	References
Pt/GO-AuNPs/Ab	0.24 fg mL^{-1}	0.001 fg mL^{-1}–0.02 µg mL^{-1}	[21]
GCE/MWCNT/His-rGO/Thionine/Ab	2.8 fg mL^{-1}	10 fg mL^{-1}–20 ng mL^{-1}	[22]
GCE/Au@thionine functionalized GO/Ab$_1$/PSA/Ab$_2$/PtCu@rGO/g-C$_3$N$_4$	16.6 fg mL^{-1}	50 fg mL^{-1}–40 ng mL^{-1}	[24]
GRP-PS$_{67}$-b-PAA$_{27}$-Au	40 fg mL^{-1}	0.1 pg mL^{-1}–100 ng mL^{-1}	[25]
Mesoporous core–shell Pd@Pt nanoparticles/amino group functionalized graphene nanocomposite	3.3 fg mL^{-1}	10 fg mL^{-1}–50 ng mL^{-1}	[26]
AuNPs/CHI/SPE	0.001 ng mL^{-1}	1–18 ng mL^{-1}	[27]
PSA/BSA/anti-PSA/AuNPs/nano-PEDOT-GA/GCE	0.03 pg mL^{-1}	0.0001–50 ng mL^{-1}	[28]
GCE/Lu-PtNPs@GS/Ab	0.3 pg mL^{-1}	1 pg mL^{-1}–10 ng mL^{-1}	[29]
3D PtCu HNFs	0.003 ng mL^{-1}	0.01–100.0 ng mL^{-1}	[30]
Ab/NH$_2$-MoS$_2$ SPEs	0.001 ng mL^{-1}	0.001–200 ng mL^{-1}	[31]
PdAuPt/COOH-rGO	2 pg mL^{-1}	3 pg mL^{-1}–60 ng mL^{-1}	[32]
Cu$_2$O@CeO$_2$-Au/GCE	0.03 pg mL^{-1}	0.1 pg mL^{-1}–100 ng mL^{-1}	[33]

Abbreviations: LOD: Limit of detection; DLR: Dynamic linear range; Ab: Antibody; GCE: Glassy carbon electrode; MWCNT: Multiwalled carbon nanotube; rGO: Reduced graphene oxide; g-C$_3$N$_4$: Graphitic carbon nitride; GRP: Graphene nanoplatelets; M-Pt/PdNPs: Mesoporous core-shell Pd@Pt nanoparticles; SPE: Screen-printed electrode; GS: graphene nanosheets; PEDOT: Poly(3,4-ethylenedioxythiophene); Lu-PtNPs@GS: Luminol functionalized platinum nanoparticles loaded on graphene nanosheets; HNFs: Hollow nanoframes.
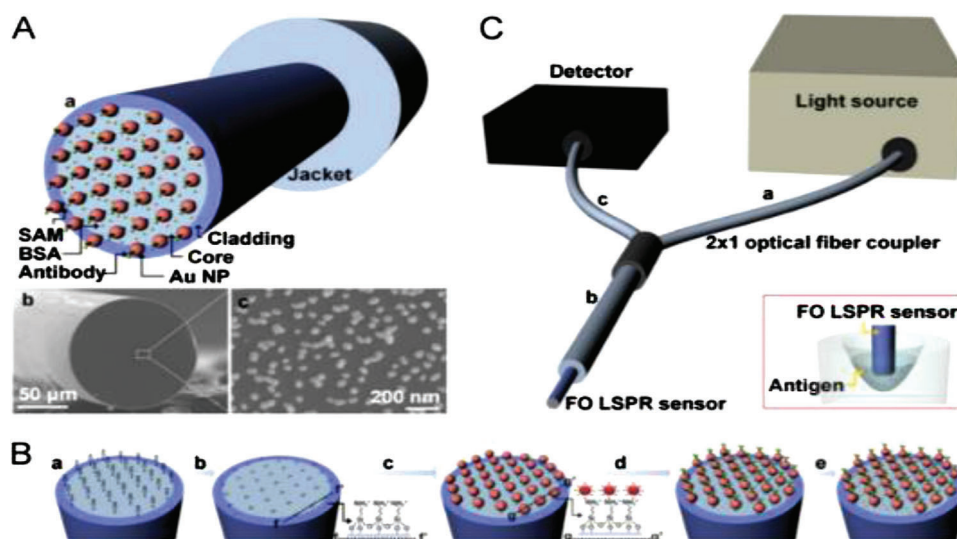

Figure 4. A) Schematic diagram of the FOLSPR sensor a), FE-SEM images of the end-face for the FOLSPR sensor b) the synthesized AuNPs on the end-face of the FO, c) SEM image of AuNPs. B) Preparation procedure of the FOLSPR sensor: a) surface functionalization with hydroxyl groups, b) creating Amine functional Groups, c) immobilization AuNPs on the SAM, d) antibody IFN-g and antibody PSA are captured on the AuNPs, e) blocking by BSA. C) illustration of the optical measurement system with the FOLSPR sensor: a) FO connector to light source, b) FO for receiving the reflected LSPR signals, c) FO for transmit signals to detector. Reproduced with permission.[38b] Copyright 2019, Elsevier.

radical prostatectomy at concentrations as low as 14 fg mL^{-1} (0.4 fM).[42]

2.2. Aptamer-Based Biosensors

Although monoclonal antibodies are widely used in cancer diagnosis, chemical antibodies, also called aptamers, show several advantages over them such as in vitro production, smaller size, reversible conformation resistance to temperature changes, non-immunogenicity, functionalization capability, stability, more

facile and economic production.[5] Aptamers consist of short single stranded DNA or RNA (ssDNA or ssRNA) molecules. Thanks to their 3D structures, which allow them to recognize a variety of targets, they have high affinity to form stable and specific complexes with the target molecule.[43] Aptamers are produced by the systematic evolution of ligands by exponential enrichment (SELEX) technique and selected through the in vitro process independent of animals or cell lines.[44] The principle is that ligands evolve systematically with reference to the glycosylation site of glycoproteins.[5] In 2019, Jolly et al. demonstrated
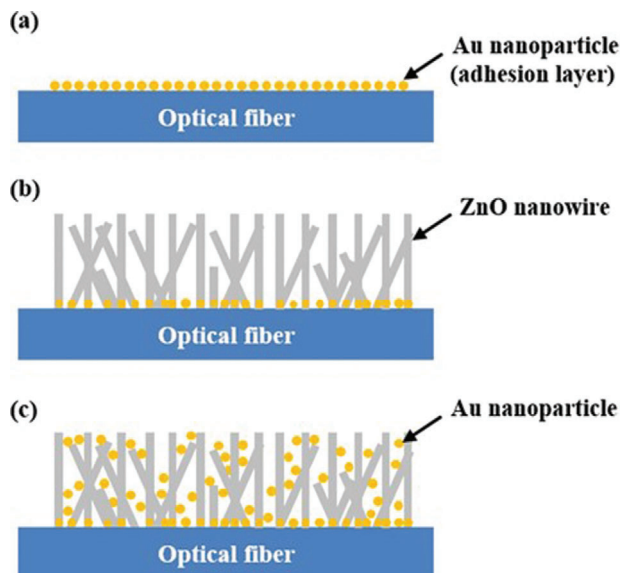
**ADVANCED
SCIENCE NEWS**

www.advancedsciencenews.com

**ADVANCED
MATERIALS
TECHNOLOGIES**

www.advmattechnol.de

Figure 5. Fabrication process of ZnO nanowires and AuNPs composite structure: a) fixation of AuNPs on optical fiber, b) growth of ZnO nanowires, and c) coating of AuNPs on ZnO nanowires. Reproduced under the terms of the CC-BY license.[41] Copyright 2019, The Authors, published by Springer Nature.

a simple strategy for preparing PSA-targeted aptamers that bind the glycan moiety of PSA (**Figure 6**). The selected aptamer was designed as an aptamer-based sandwich format sensor to detect PSA with an LOD of 10 pg mL^{-1}.[45] A dual mode impedimetric and amperometric aptasensor was developed by using either 6-mercapto-1-hexanol (MCH) or 6-(ferrocenyl) hexanethiol (FcSH) to immobilize the anti-PSA DNA aptamer on the surface of AuNPs (**Figure 6**). This dual detection method may reduce false positives and provide additional validation of the signals.[45] Another screen-printed carbon electrode (SPCE) was modified by AuNPs conjugated to thiolated aptamers (**Figure 7**) and the aptasensors LOD was reported to be 0.077 pg mL^{-1}.[46] In addition to AuNPs, other nanomaterials that can amplify the signal intensity are also used in the modification of aptasensor. Among carbon nanomaterials, GO, graphene nanocomposites and single-wall carbon nanotubes (SWCNT) are often used as electrode matrices or conductive materials for biosensors because of their large surface area and excellent conductivity and stability.[47] Wei et al. developed a DNA aptamer-based electrode that was modified by AuNPs /reduced graphene oxide (rGO)/thionine (THI) nanocomplexes. It had the advantage of fast response time and low cost with an LOD of 10 pg mL^{-1}.[48] Recently, a GO aptamer coupling material synthesized by combining integrated aptamers with GO has been reported to be a better option for cancer diagnostic and therapeutic strategies.[49] Thanks to hydrophobic/π-stacking interactions, GO can easily bind to the single-stranded aptamer. This GO aptamer coupling material is also widely used in electrochemical aptasensors and fluorescence aptasensor. In 2021, Shahbazi Toloun et al. investigated the stability and interaction mechanism of the aptamer with PSA and SWCNT using computational techniques and proposed the hypothesis that the 3D structure of the aptamer remains stable in the presence of PSA proteins and SWCNT.[50] However, the

study would be more interesting if it included how to immobilize the SWCNT on the electrode base and compared the maximum space utilization per unit area of SWCNT with that of MWCNT.

In the literature there are many examples of DNA aptamer-PSA specific interaction applied in LSPR sensors. In 2018, Khan et al. developed an LSPR extinction spectrum based on gold nanoarrays specifically adapted to PSA aptamers.[51] Its advantage over other commonly used PSA biosensors is that the use of specific aptamer functionalized AuNPs for PSA increased the stability of AuNPs and improved their interaction with PSA. Moreover, the recovery of the substrate was also successfully demonstrated by Khan et al. Another nanostructured biosensing platform was designed by Duan et al.[52] First, a 2D nanocomposite was formed by graphitic carbon nitride (g-C$_3$N$_4$) nanosheets and MoS$_2$ quantum dots (MoS$_2$ QDs). CHIT-stabilized Au nanoparticles (CHIT-AuNPs) were prepared by plasma enhanced-chemical vapor deposition and decorated on the MoS$_2$ QDs sheet. Finally, the 2D MoS$_2$QDs@g-C$_3$N$_4$@CHIT-AuNPs platform was simultaneously employed as both an SPR sensor and electrochemical aptasensor with satisfactory LODs of 0.77 ng mL^{-1} and 0.71 pg mL^{-1} respectively. Data from several studies suggest that g-C$_3$N$_4$ is a low-cost, environmentally friendly semiconductor material that can be used as a large scaffold for nanocomposites.[53,54] MoS$_2$ nanostructures are also widely used in PSA biosensors because of their electronic properties, which are highly sensitive and selective.[31,55] Duan et al. concluded that when the advantages of the three components are combined, the MoS$_2$QD@g-C$_3$N$_4$@CHIT-AuNPs-based aptasensor exhibits high sensitivity, low LODs, stability, and reproducibility and a proposed strategy capable of potential applications in clinical diagnostics or immune research.[52]

As shown in **Table 3**, for the construction of sensitive and highly selective platform biosensors, the greatest advantage of aptamers over antibodies is that they can be chemically modified and can bind to different labels, which gives them the opportunity to be modified on a wider range of potential nanomaterials.

2.3. Peptide-Based Biosensors

The application of peptides in different PSA detection biosensors depends upon the detection principle employed. When peptides are used as recognition elements, they are similar to antigen-antibody and receptor-ligand reactions, but they have a simpler structure and are therefore modified by chemical targeting.[56] At the same time, peptides have a smaller spatial structure than antibodies and therefore can reduce the steric hindrance effects and improve the detection sensitivity of biosensors.[57] The different roles of peptides in the design of electrochemical biosensors for clinical diagnostics is reported recently by Sfragano et al.[58] Most researchers investigating PSA peptide-based biosensors have utilized the technique of electrochemical peptide-cleavage. First, peptides can be produced rapidly and in large quantities by in-vitro display technology, then immobilized at the electrode surface by covalent or amino bonds and the electrochemical signal is measured by connecting electrochemical active agents (e.g., ferrocene (Fc) and methylene blue (MB)). Finally, in the presence of PSA, the peptides are specifically recognized and cleaved, resulting in a change in the electrochemical signal used to detect PSA.
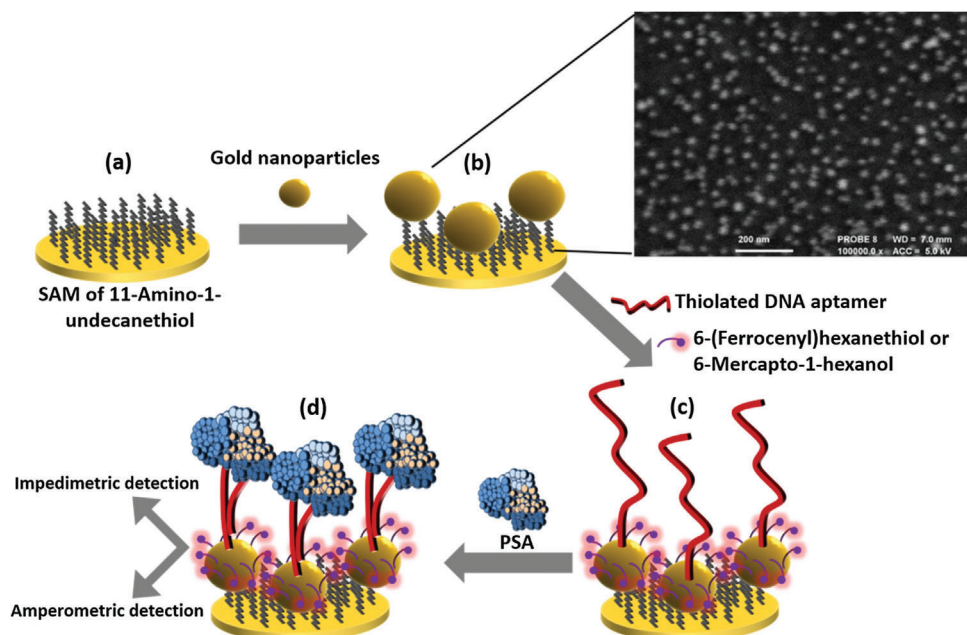
ADVANCED
SCIENCE NEWS

www.advancedsciencenews.com

ADVANCED
MATERIALS
TECHNOLOGIES

www.advmattechnol.de

Figure 6. Schematic of the AuNP-modified aptasensor showing how either impedimetric or amperometric detection can be used depending on whether the DNA aptamer is co-immobilised with MCH or FcSH. Reproduced with permission.[45] Copyright 2017, Elsevier.
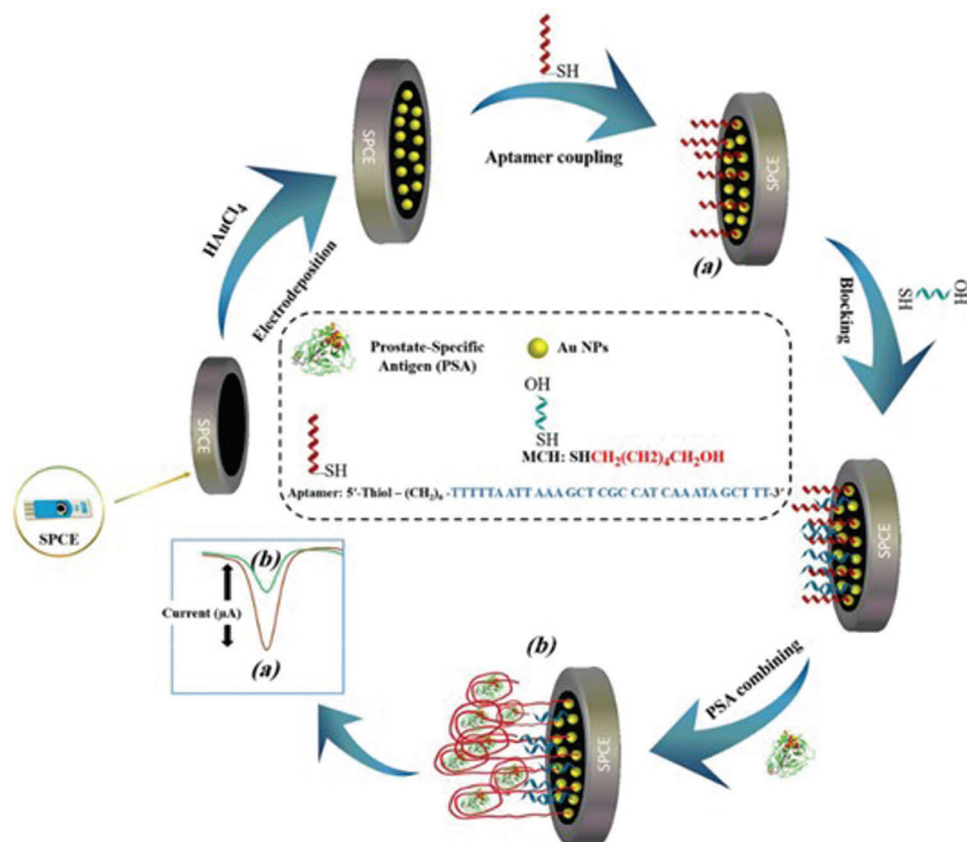

Figure 7. Schematic illustration of PSA assay based on the electrochemical technique. Reproduced under the terms of the CC BY-SA license.[46] Copyright 2020, The Authors, published by Frontiers Media.

Table 3. Comparison of ELISA and biosensing techniques for the determination of tumor markers.[46].

| Techniques	Conventional method [ELISA]	Electrochemical Aptasensor
Biorecognition element	An antibody is expensive and needs complex reactors. Storage: Needs to freeze.	An aptamer is inexpensive and chemically synthesized. Storage: Stable at room temperature
Sample preparation and reagent	More organic solvent consumption, higher sample volume, more reagent, and higher cost	Less organic solvent consumption, lower sample volume, less reagent, and lower cost
Analysis and application	Centralized laboratories with experienced personnel	Portability and no expertise required
Assay time	Time-consuming	Rapid real-time determination
Specificity and selectivity	Matrix interface problem Possible false positive/negative results	High selectivity and specificity for tumour marker determination
Analytical apparatus price	Expensive	Inexpensive
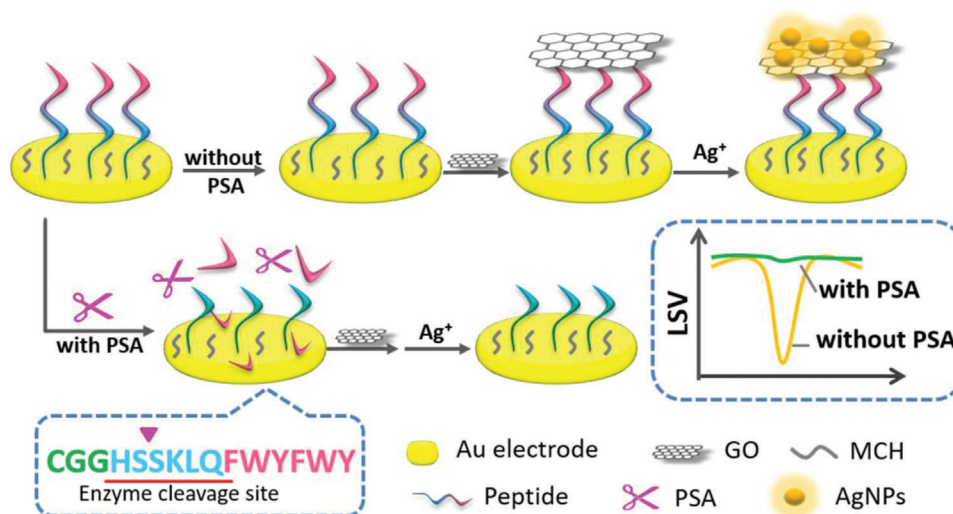
Figure 8. Schematic illustration of the peptide cleavage-based electrochemical biosensor for the detection of PSA. Reproduced with permission.,[59] Copyright 2019, Elsevier.

Meng et al. demonstrated a specific peptide working on a gold electrode as a molecular recognition element for the induction of PSA antigen (**Figure 8**).[59] GO with AuNPs were immobilized at the other end of the peptide. In the absence of PSA, the reduction reaction triggered by the aggregation of silver ions would form silver nanoparticles (AgNPs) and accordingly generate an electrical signal peak. However, when PSA was added, one of the sequences in the peptide is specifically recognized and cleaved, so that AgNPs cannot be formed leading to a significant decrease in electrochemical response. The LOD of this peptide cleavage-based electrochemical biosensor for PSA was 0.33 pg mL^{-1}.[59] Similarly, another GO nanocomposite, graphene oxide-Fe$_3$O$_4$-thionine (GO-Fe$_3$O$_4$-Thi), was applied to a peptide cleavage-based biosensor developed by Ding et al.[60] Compared with AuNPs, GO-Fe$_3$O$_4$-Thi composite nanomaterials can be used not only as peroxidase mimic but also as electrochemical probes to measure the concentration of PSA. The uncut sequences tagged with Fc can be used as an internal reference to ensure the reliability and accuracy of the measurement. The LOD of this dual-mode PSA biosensor was 0.76 (DPV) and 0.42 (CA) pg mL^{-1} (further discussed ahead). Although there are few studies on the interaction of peptides with GO (peptide functionalized graphene derivatives), the formation of GO-peptide conjugate with large surface area and enhanced chemical stability at high temperatures has been reported.[61] In addition to GO, molybdenum has been widely studied as a transition metal dichalcogenide (TMD) nanomaterial because of its novel properties. The coupling of graphene and MoS$_2$ has been the most interesting in recent years, and synergistic effects of this composite nanomaterial have been reported to exceed the properties of each nanomaterial alone, for example, when GO is combined with MoS$_2$, GO-MoS$_2$ performs better than graphene alone in terms of electron transfer and electrochemical signals.[62] Another study on peptide-based PSA biosensors adopted molybdenum diselenide@reduced graphene oxide (MoSe$_2$@rGO) nanocomposite to modify the electrode surface, then AuNPs and MoSe$_2$@rGO were connected to each other by Au-S bonds, finally a magnetic DNAzymepeptide-Fe$_3$O$_4$ probe was prepared and attached to the AuNPs via amino bonds. The LOD of this PSA biosensor was 0.3 fg mL^{-1} (**Figure 9**).[63] Together, these studies provide important insights into composite nanomaterials composed of GO and molybdenum. However, many researchers now argue that the strategy of TMDCs used in biosensors has not been successful. The problem of toxic gases released by composite
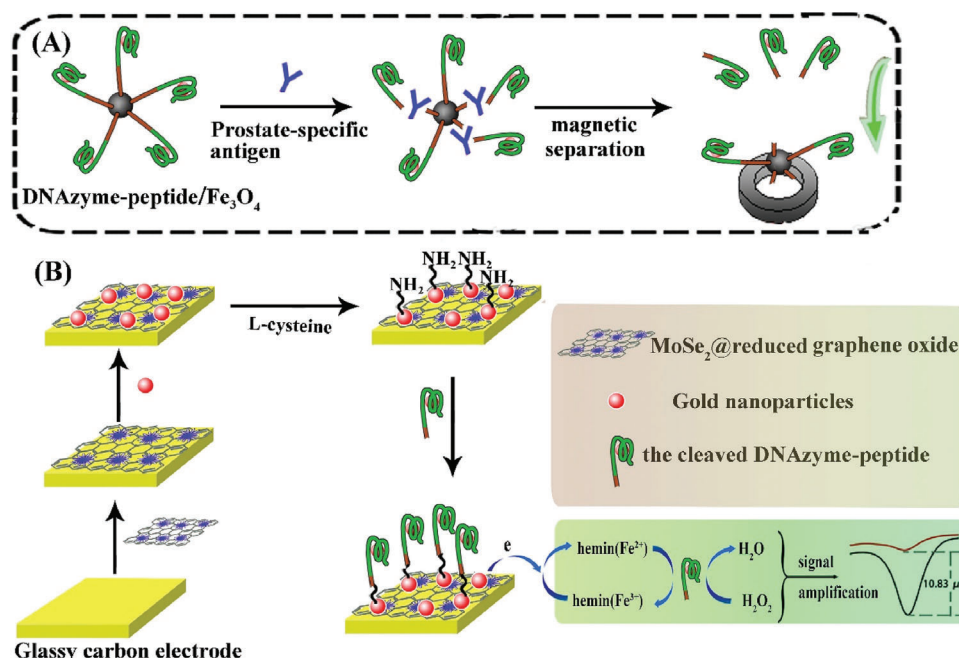
**ADVANCED
SCIENCE NEWS**

www.advancedsciencenews.com

**ADVANCED
MATERIALS
TECHNOLOGIES**

www.advmattechnol.de

Figure 9. Schematic illustration for the preparation of DNAzyme-peptide/Fe$_3$O$_4$ probe and "signal-on" electrochemical peptide biosensor based on the versatile magnetic probe. Reproduced with permission.[63] Copyright 2020, Elsevier.

nanomaterials composed of MoS$_2$, etc. for biosensing cannot be ignored.[64]

With the intensive research on peptide-based biosensors, the development of nanocomposites with good conductivity and excellent probes for anchoring peptides to capture electrochemical signals has received increasing attention (**Table 4**). In 2021, Xu et al. designed MXene loaded AuNPs and MB nanocomposites (MXene-Au-MB) immobilized on a GCE surface (**Figure 10**). MXene is prepared by the reaction of Ti$_3$AlC$_2$ and HF solution. MXene has a strong reducing ability and can reduce metal nanoparticles (e.g., AuNPs, AgNPs) without the addition of reducing agent and stabilizer. The probe is made of carboxy-modified Fc, which not only binds to peptides but also can resist non-specific adsorption to complex samples.[65]

In 2022, Hui et al. developed an ultra-low contamination high-sensitivity biosensor with anti-contamination peptides and signal amplification strategies (**Figure 11**, Left).[66] First, PEG/PEDOT nanocomposites were electrodeposited onto the electrode surface using cyclic voltammetry (CV). Second, streptavidin was incubated in NHS and EDC solutions and immobilized on PEG/PEDOT surface. Then, a set of peptides containing sequences recognizable by PSA are immobilized on the PEG/PEDOT through the interaction of labelled biotin with streptavidin. Finally, the DNA-functionalized AuNPs were bound to the sulfhydryl-terminated peptides via Au–S bonds and adsorbed electroactive MB. Its antifouling properties are mainly reflected in the antifouling zwitterionic domain, and the PSA-induced cleavage domain designed by the peptide chain.

Table 4. Summary of selected nanomaterials based peptisensors for the prostate-specific antigen (PSA) detection.

Nanostructure/Strategy	Detection technique	Detection range	LOD	References
Peptide and GO/AgNPs	LSV	5 — 2×10^4 pg mL^{-1}	0.33 pg mL^{-1}	[59]
Peptide-conjugated hemin/G4 and MoSe$_2$@rGO nanocomposites	DPV	1 fg mL^{-1}–80 ng mL^{-1}	0.3 fg mL^{-1}	[63]
FPANs	Fluorescent	10 pM–100 nM	10 pM	[67]
CNTs/GO and Peptide-Cu(II) complex	LSV	10 pg mL^{-1}–2 ng mL^{-1}	10 pg mL^{-1}	[68]
GCE/CNT-PAMAM/GA/β-CD electrode	DPV	0.001–30 ng mL^{-1}	0.78 pg mL^{-1}	[69]
AuNPs/peptide/BSA/DSP/depAu/GCE	EIS	0.2 pg mL^{-1}–45 ng mL^{-1}	0.06 pg mL^{-1}	[70]
DSP@Au@SiO$_2$/peptide/MWCNTs–PAMAM/GC	LSV	0.001–30 ng mL^{-1}	0.7 pg mL^{-1}	[71]
Ru(bpy)$_3$$^{2+}$/AuNPs/Nafion/GCE	ECL	5 pg mL^{-1}–5 ng mL^{-1}	0.8 pg mL^{-1} (or 8×10^{-13} g mL^{-1})	[72]

Abbreviations: CV: Cyclic voltammetry; LSV: Linear sweep voltammetry; DPV: Differential pulse voltammetry; EIS: Electrochemical impedance spectroscopy; GCE: Glassy carbon electrode; CNTs: Carbon nanotubes; PAMAM: Poly(amidoamine): ECL: Electrochemiluminescence; FPANs: Fluorescein isothiocyanate (FITC)/peptide-conjugated gold (Au) nanoparticle complexes; DSP: Dithiobis(succinimidyl propionate); AuNPs: Gold nanoparticles.
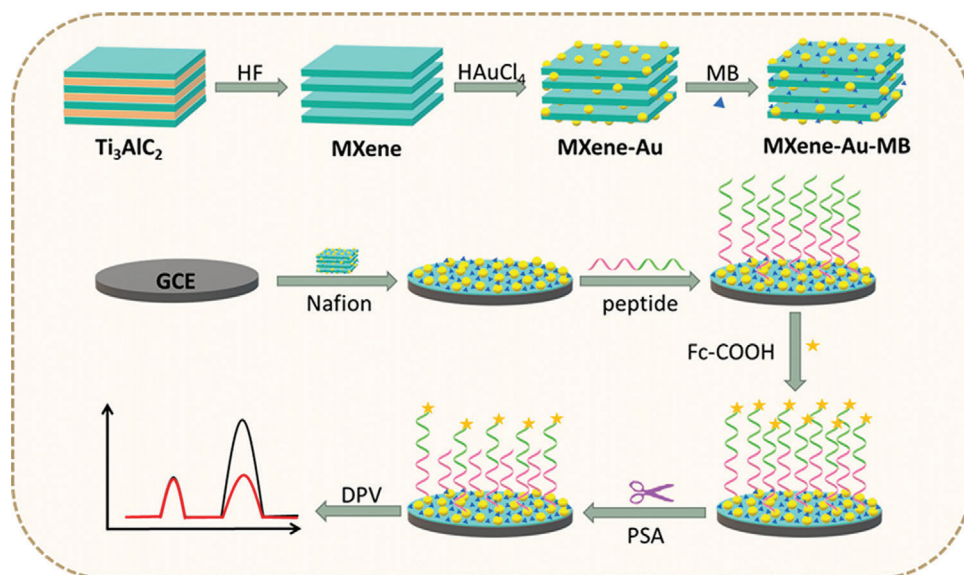
**ADVANCED
SCIENCE NEWS**

www.advancedsciencenews.com

**ADVANCED
MATERIALS
TECHNOLOGIES**

www.advmattechnol.de

Figure 10. Schematic illustration of Ratiometric Antifouling Electrochemical Biosensor Working Mechanism. Reproduced with permission.[65] Copyright 2021, American Chemical Society.
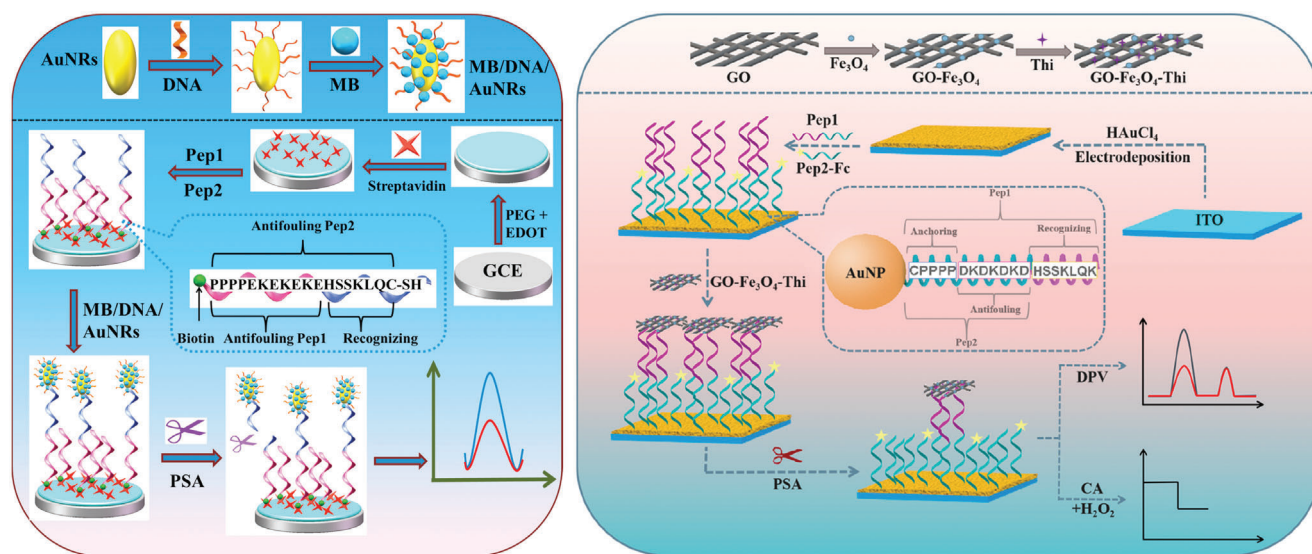

Figure 11. Left: Schematic diagram and working principle of the antifouling electrochemical biosensor. Reproduced with permission.[66] Copyright 2022, Elsevier. **Right**: Scheme for antifouling electrochemical biosensor working principle. Reproduced with permission.[60] Copyright 2019, American Chemical Society.

In addition, the PEG/PEDOT platform provides a 3D porous substrate with large electroactive surface area, excellent electrical conductivity, and antifouling ability. Biosensor exhibited a LOD of 0.035 pg mL^{-1} and linear range from 0.10 pg mL^{-1} to 10.0 ng mL^{-1}.[66]

Ding et al. (2019) reported a dual-mode and low fouling (antifouling) electrochemical PSA biosensor based on antifouling peptides loaded with internal references and electrochemical probes (Figure 11, Right).[60] The PSA detection was based on two kinds of antifouling peptides functionalized with a GO−Fe$_3$O$_4$−thionine (Thi) probe and an internal reference Fc.

The longer peptide (Pep1) modified with the probe (GO-Fe$_3$O$_4$-Thi) was designed to contain a peptide sequence (HSSKLQK) capable of being recognized and cut by the PSA. The GO-Fe$_3$O$_4$-Thi probe functions as a peroxidase mimic (GO-Fe$_3$O$_4$) and an electrochemical probe due to the presence of Thi. Thi provided a sensitive current response originating from its redox reaction using differential pulse voltammetry (DPV) and GO-Fe$_3$O$_4$ with good catalytic ability for H$_2$O$_2$ reduction produced an enhanced chronoamperometry (CA) signal, while the Fc as internal reference ensured the reliability and accuracy of the assay. The excellent antifouling ability due to the presence of antifouling
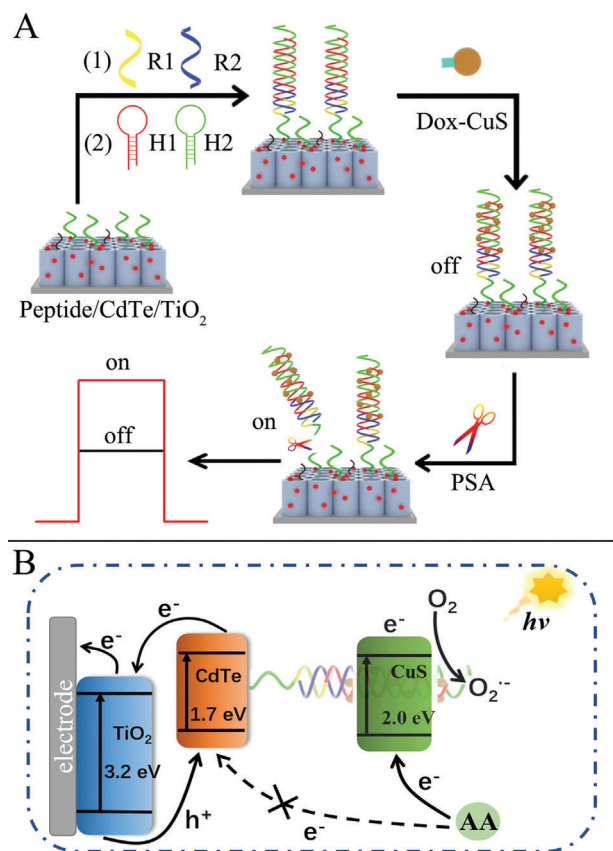
**ADVANCED
SCIENCE NEWS**

www.advancedsciencenews.com

**ADVANCED
MATERIALS
TECHNOLOGIES**

www.advmattechnol.de

Figure 12. Schematic diagram of the construction A) and the response mechanism B) of PEC biosensor. Reproduced with permission.[74] Copyright 2020, Elsevier.

zwitterionic peptides on the sensing interface, makes this assay a highly attractive method for the detection of PSA in human serum samples. The dual-mode PSA sensor exhibited a wide linear range from 5 pg mL^{-1} to 10 ng mL^{-1}, with low LOD of 0.76 and 0.42 pg mL^{-1} through DPV and CA modes, respectively. Table 4 summarizes some of the best selected peptisensors based on the nanomaterials for determination of PSA tumor marker.

While a large and growing body of literature has investigated electrochemical biosensor, there is a relatively small body of literature that is concerned with the development of fluorescence biosensor and photoelectrochemical biosensor. Yang et al. presented a novel peptide/Fe$_3$O$_4$@SiO$_2$-Au nanocomposite fluorescence biosensor for the first time. 5-carboxyfluorescin (5-FAM) labelled peptide was prepared on the surface of Fe$_3$O$_4$@SiO$_2$-Au magnetic nanocomposite, resulting in quenching of the FAM fluorescence. PSA specifically recognized and cleaved the 5-FAM labelled peptide, resulting in fluorescence recovery.[73] Magnetic nanomaterials composed of Fe$_3$O$_4$ and SiO$_2$ with excellent salt stability and dispersibility were reported to effectively quench FAM-peptide, which had an LOD of 3.0×10^{-13} g mL^{-1} (0.3 pg mL^{-1}).

In another study, Zhao et al. constructed a peptide-based photoelectrochemical biosensor for PSA detection (**Figure 12**).[74] Peptide chains containing sequences recognizable by PSA were attached to the CdTe/TiO$_2$ surface in the presence of NHS and

EDC. The other end of the peptide chain was immobilized by double-helix DNA as a carrier for doxorubicin-copper sulfide nanocrystals (Dox-CuS). This article states that the photoelectrochemical biosensor had good specificity, stability, and reproducibility with an LOD of 0.0015 ng mL^{-1} with a linear range from 0.005 – 20 ng mL^{-1}.

Peptide-based biosensors have several advantages including low LODs. However, some challenges remain in terms of their analytical performance. One such issue is non-specific cleavage of the enzymatic sites that can reduce peptide-based biosensor accuracy. An important milestone in their development has been the development of antifouling peptide-based biosensors but it still has a long way to go for commercial application.

2.4. Nanopore-Based Biosensors

Chuah et. al. demonstrated nanopore blockade sensors for ultrasensitive detection of proteins in complex biological samples. Antibody-modified magnetic nanoparticles ((anti-PSA)-MNPs) that diffuse at zero magnetic field to capture PSA.[75] The (anti-PSA)-MNPs were magnetically driven to block an array of nanopores rather than translocate through the nanopore. Specificity was obtained by modifying nanopores with anti-PSA antibodies such that PSA molecules captured by (antiPSA)-MNPs form an immunosandwich in the nanopore. Reversing the magnetic field removes (anti-PSA)-MNPs that have not captured PSA thereby limiting non-specific effects. The combined features allowed detecting PSA in whole blood with a 0.8 fM detection limit (**Figure 13**).[75]

Wu et al. demonstrated the development of an ultrasensitive nanopore blockade biosensor that can rapidly diagnose PSA with high selectivity (**Figure 14** (Top)).[76] The solid-state nanopores had gold located only along the length of the nanopore while the rest of the membrane was silicon nitride. The orthogonal use of materials allowed nanopore arrays with a different surface chemistry inside the nanopore relative to the rest of the membrane to be fabricated that improved the detection limit of nanopore blockade sensors in quantitative analysis. Based on such functionalized nanopore devices, nanopore blockade sensors lower the detection limit by an order of magnitude and enable ultrasensitive detection of PSA as low as 80 aM.[76] Lin et al. designed a solid-state nanopore sensor for the direct sensing and quantification of PSA as cancer biomarker in serum without any pre-treatment for a convenient quantification of cancer biomarkers in clinical samples: PSA in serum samples that could be determined as low as ≈1 pM, within 30 min (Figure 14 (Bottom)).[77]

3. Sarcosine Oxidase-Targeted Biosensors

Sarcosine (*N*-methylglycine) is considered a potential non-invasive prostate cancer specific biomarker and has been widely used in biosensing. It is an amino acid that occurs naturally in the body and is readily detectable in the urine of patients. Normally, the concentration of sarcosine in the blood of healthy individuals is 1.4 ± 0.6 μM and in the blood of prostate cancer patients is 2–10 μM. In the presence of H$_2$O and O$_2$, the enzyme sarcosine oxidase (SOx) catalyses the conversion of sarcosine to

**ADVANCED
SCIENCE NEWS**
www.advancedsciencenews.com

**ADVANCED
MATERIALS
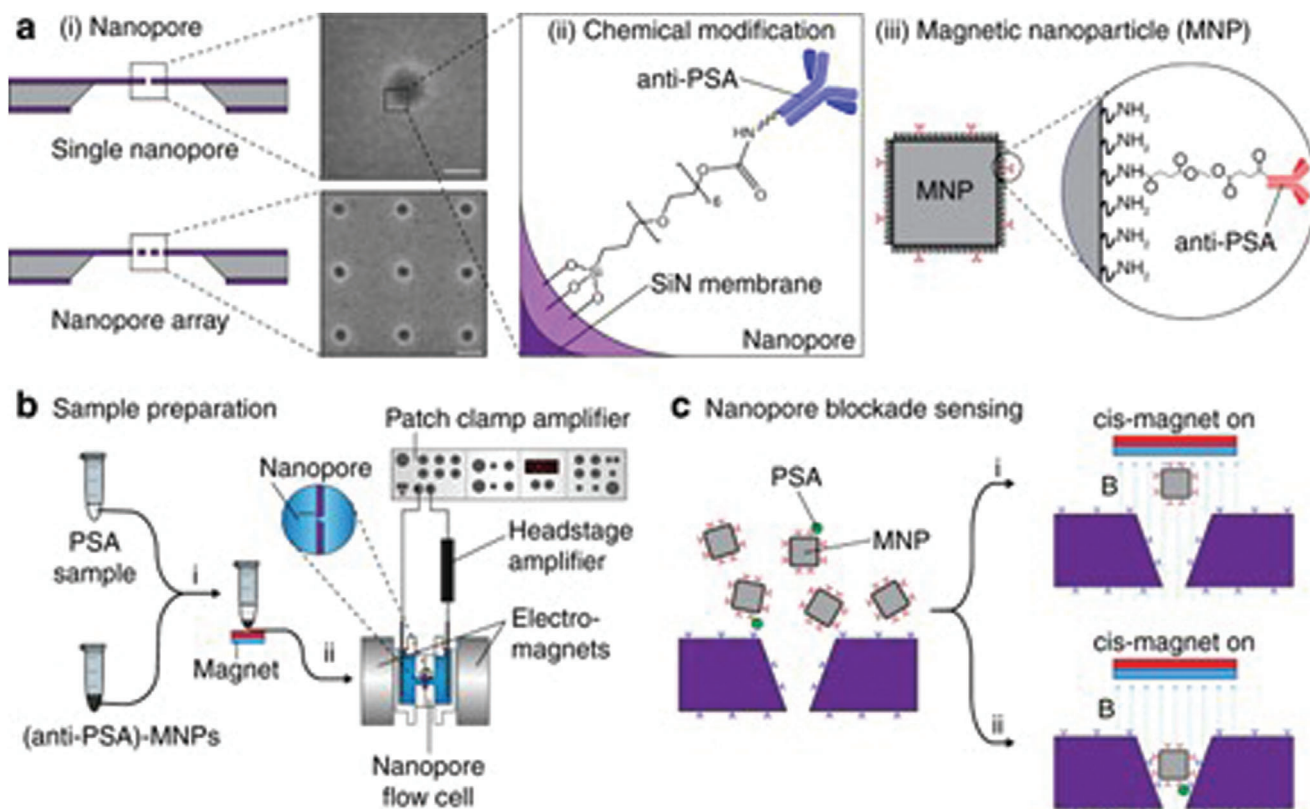TECHNOLOGIES**
www.advmattechnol.de

Figure 13. Nanopore blockade sensor. a) (i) Schematics and scanning electron micrographs of (top) a solid-state nanopore, inset: a 48 nm nanopore, scale bar: 100 nm; (bottom) a nanopore array in SiN membrane, inset: a 3 × 3 array of nanopores with 0.5 µm spacing between each pore, scale bar: 200 nm. (ii) Illustration of a chemically modified SiN nanopore with silane-EG$_6$-(anti-PSA) self-assembled monolayer (SAM); EG equates to ethylene glycol. (iii) Illustration of an (anti-PSA)-conjugated MNP used. Inset: chemical structure of the (anti-PSA)-EG$_6$ immobilized onto the amine-rich PEI coating of the MNP. b) Flow chart illustrates the sample preparation steps for detection of PSA in a sample. (i) Sample containing PSA was mixed with (anti-PSA)-MNPs. After exposing the MNPs to the sample, the MNPs were then magnetically separated and washed 3 times with PBS. (ii) The MNPs were subsequently added into the cis-chamber of a nanopore flow cell filled with KCl as electrolyte. A potential difference was applied between both sides of the nanopore. c) Active filtering of non-specific nanopore blockade events can be achieved by applying a magnetic field from the cis-side. (i) (Anti-PSA)-MNP that non-specifically adsorbed onto the pore surface will be ejected and thus unblocks the pore, whereas (ii) (anti-PSA)-MNP that contains captured PSA will continue blocking the pore. Blue dashed lines represent the magnetic field lines, B. Reproduced under the terms of the CC-BY license.[75] Copyright 2019, The Authors, published by Springer Nature.

glycine with H$_2$O$_2$ generated from the reaction further oxidized at the electrode surface. In recent years, several sensor systems using AuNPs have been developed for the construction of reaction frameworks for sarcosine.[78–80] V. Narwal et al. constructed an amperometric sarcosine biosensor based on the covalent immobilization of SOx (or SarOx) on a nanocomposite of carboxylated multi-walled carbon nanotubes (cMWCNT)/chitosan (CHIT) and copper nanoparticles (CuNPs) and electrodepositing onto Au electrodes (CHIT/CuNPs/c-MWCNT/AuE, **Figure 15**).[78] Biosensor showed optimum current at 0.5 V (pH = 7.0 & T = 35 °C). The working range of biosensor was 0.1–100 µM with LOD of 0.1 pM and high storage stability (180 days) reported (Figure 15).[78] Same group, Kumar et al. reported a similar work by constructing an amperometric sarcosine biosensor (SOxNPs/AuE) for detection of prostate cancer, and LOD (0.01 µM) and response time (2 s) were achieved. Authors claimed that SOxNPs/Au electrode lost only 10% of its initial activity after 180 days (storage at 4 °C).[79] Same group, R. Deswal et al. constructed an improved amperometric sarcosine biosensor using Au electrodes

(SOx/CHIT/GNRs/Au, **Figure 16**).[80] Despite simplifying the preparation of nanocomposite-based enzyme electrodes, they noted that the current work lacked miniaturization, therefore pointing to need for additional research focusing on miniaturization. The biosensor covalently immobilizes SOx on a nanocomposite of CHIT and graphene nanoribbons (GNRs) deposited on an Au electrode. Authors claimed that the biosensor showed linearity in the range of 0.001–100 µM with a LOD of 0.001 µM.

Furthermore, magnetic nanoparticle-based biosensing strategies have received a lot of attention due to their affordability and high physical and chemical stability. In 2018, D. Uhlirova et al. successfully applied superparamagnetic iron oxide nanoparticles (SPIONs) to the modification of CHIT and SOX (SPIONs/Au/CS/SOX/NPs, **Figure 17**).[81] The report states that CHIT is one of the most commonly used biopolymers for immobilizing biomolecules due to its excellent film-forming ability, high permeability, ease of chemical modification, high mechanical strength, non-toxicity, and low cost. After testing, they also concluded that the system's low cost and reproducibility offer
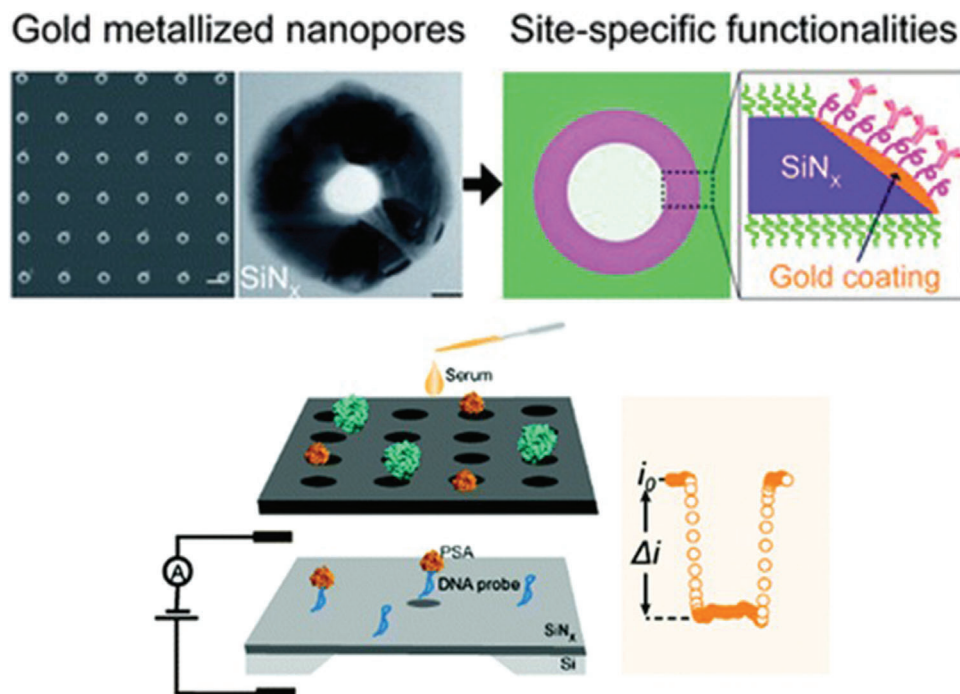
**ADVANCED
SCIENCE NEWS**

www.advancedsciencenews.com

**ADVANCED
MATERIALS
TECHNOLOGIES**

www.advmattechnol.de

Figure 14. Top: Selectively detecting attomolar concentrations of proteins using gold lined nanopores in a nanopore blockade sensor. Reproduced under the terms of the CC-BY license.[76] Copyright 2020, The Authors, published by The Royal Society of Chemistry. **Bottom**: Direct sensing of cancer biomarkers in clinical samples with a designed nanopore. Reproduced with permission.[77] Copyright 2017, The Royal Society of Chemistry.

advantages in the development of miniaturized POC technologies. LOD of 5 μM was reported and suggested method was further validated for artificial urine analysis (LOD 18 μM).

It is obvious that the development of SOx-based biosensors is still in its infancy compared to the PSA-based electrochemical biosensors. One of the breakthroughs is to investigate suitable and efficient nanomaterials for immobilizing SOx. In 2020, Stefania Hroncekova's team developed a 2D layered nanomaterial Ti_3C_2TX (a member of the MXene family) to immobilize SOx. It was shown that MXene material bound to CHIT was a sensitive immobilization carrier, and biosensor reported with a LOD

of 18 nM and a linear range up to 7.8 μM (**Figure 18**).[82] Authors concluded that since sarcosine is also present in urine, the composition of which is easier to analyze compared to human serum, sarcosine can be quantified indirectly by detecting H_2O_2 generated from the enzymatic reaction by amperometric assay.[82] To date, a limited number of MXenes-based biosensors have been developed, but the device remains a potential future electrochemical biosensing platform for protein biosensors.

Q. Yang *et al* (2019) reported a hollow magnetic Pt-Fe_3O_4@C nanocomposite with good electron transfer capability was developed for the construction of a sarcosine biosensor.[83] It was
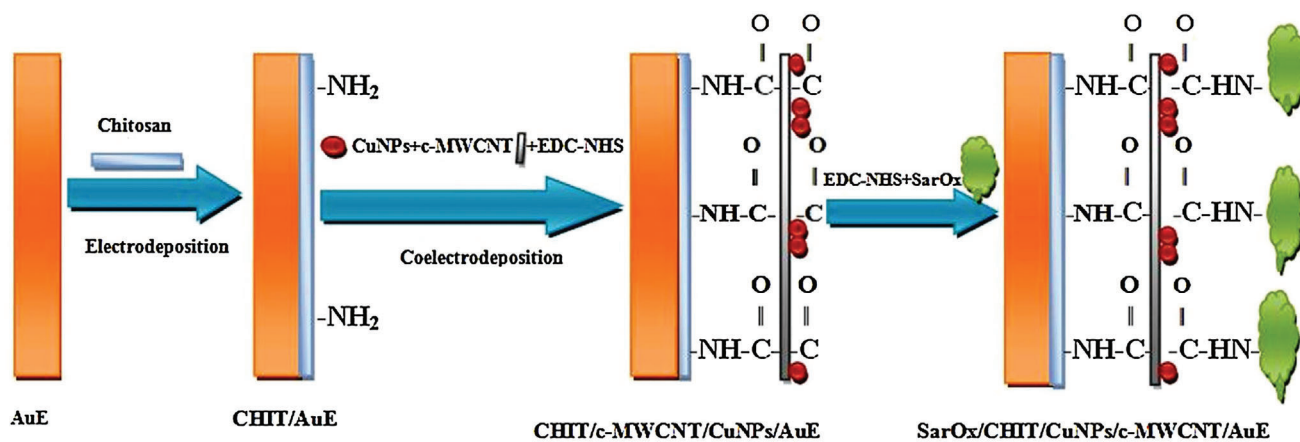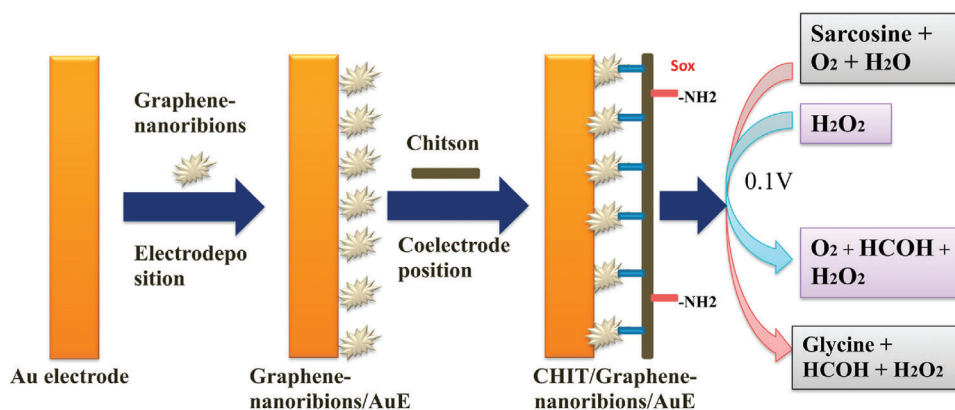

Figure 15. Schematic representation of chemical reactions involved in the fabrication of SarOx/CHIT/CuNPs/c-MWCNT/AuE. Reproduced with permission.[78] Copyright 2018, Elsevier.

**ADVANCED
SCIENCE NEWS**

www.advancedsciencenews.com

**ADVANCED
MATERIALS
TECHNOLOGIES**

www.advmattechnol.de

Figure 16. Schematic representation of fabrication of sarcosine biosensor based on SOx/CHIT/GNRs/AuE. Reproduced with permission.[80] Copyright 2022, Elsevier.
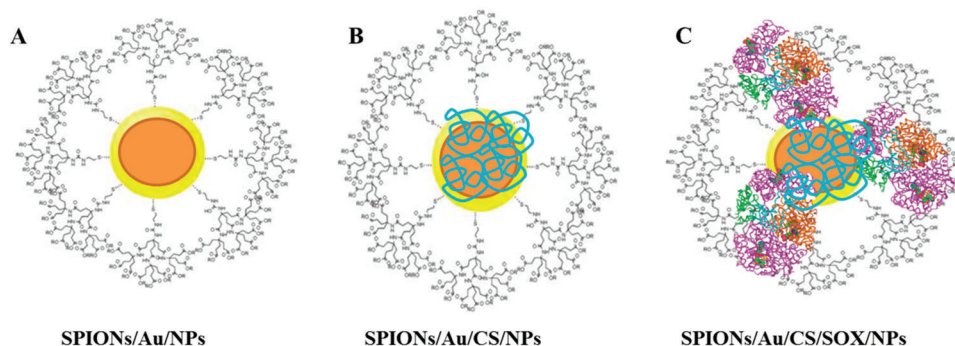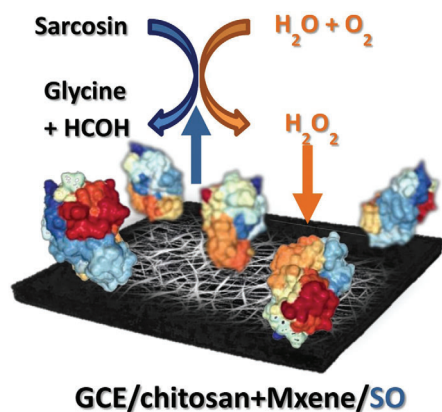

Figure 17. Scheme of prepared superparamagnetic iron oxide nanoparticles (SPIONs). A) SPIONs/Au/NPs with the surface modified with citric acid; B) SPIONs/Au/CS/NPs modified with chitosan (CS); C) SPIONs modified with CS and sarcosine oxidase (SOX)—SPIONs/Au/CS/SOX/NPs. Reproduced under the terms of the CC-BY license.[81] Copyright 2018, The Authors, published by MDPI.

Figure 18. MXene-based enzymatic biosensor (GCE/Chitosan+MXene/SOx) for detection of sarcosine. Reproduced under the terms of the CC-BY license.[82] Copyright 2020, The Authors, published by MDPI.

composed of hollow Fe_3O_4 nanospheres as a carrier for dispersed Pt nanoparticles. Then polyaniline was encapsulated on Pt-Fe_3O_4 nanoparticles, and finally the polyaniline was cleaved to carbon. The Pt-Fe_3O_4@C nanocomposite was reported to have high catalytic activity and stability. The biological activity of immobilized SOx can be greatly retained by immobilizing SOx on Pt-Fe_3O_4@C with an LOD of 0.43 μM and linear detection range between 0.5–60 μM reported.[83]

Table 5, presents a summary of nanomaterials-based sarcosine biosensors for determination of prostate cancer. The development of sarcosine biosensors is still in its early stage, but research and development of sarcosine-based biosensors has a promising future. There are many common nanomaterials such as c-MWCNT, etc. that have been employed. Compared to PSA detection-based biosensors, sarcosine-based biosensors are simpler in principle, more responsive and have competitive detection limits. The breakthrough point is the miniaturization and commercialization of their scale.

4. Other Biomarkers-Based Biosensors (Including Dual-Biomarkers Biosensors)

Other common biomarkers discussed here are PCA3, VEGF, and PSMA. Soares et al. recently (**Figure 19**) reported the first

ADVANCED
SCIENCE NEWS
www.advancedsciencenews.com

ADVANCED
MATERIALS
TECHNOLOGIES
www.advmattechnol.de

Table 5. Summary of selected nanomaterials-based sarcosine biosensors for detection of prostate cancer.

Strategy/composition of transducer of sarcosine biosensor	Range [μM]	LOD [μM]	References
SarOx/CHIT/CuNPs/c-MWCNT/Au electrode	0.1–100	1.0×10^{-7} (or 0.1 pM)	[78]
SOxNPs/AuE	0.1–100	0.01	[79]
Pt-Fe$_3$O$_4$@C/GCE	0.5–60	0.43	[83]
SOX/SPE	0.01–0.1 (10–100 nM)	0.016 (16 nM)	[84]
SOxENs/PB/SPCE	10–400	0.66	[85]
SOx/PEDOT-IA/Pt/MnPO$_4$/GCE	1–55	0.11	[86]
SOX/AgNPs/graphene–chitosan/GCE	1–177	1.0	[87]
SOx/Pt@ZIF8/Nafion	5–30	1.06	[88]
SOx/Pt/MNP/GCE	5–40	0.24	[89]
SOx/Pt/g-C$_3$N$_4$/GCE	2–70	0.8	[90]

Abbreviations: PB: Prussian blue; SPCE: Screen-printed carbon electrode; ZIF8: Porous zeolitic imidazolate framework-8; MNP: Mesoporous nickel phosphonate; CHIT: Chitosan; SPE: Screen printed electrode; g-C$_3$N$_4$: Graphitic phase carbon nitride.

electrochemical and impedance-based biosensor that are capable of detecting PCA3 made using a layer of PCA3-complementary single-stranded DNA (ssDNA) probe, immobilized on a layer-by-layer (LbL) film of CHIT and carbon nanotubes (MWCNT).[91] The biosensor showed high selectivity to PCA3, which was confirmed by impedance measurements and polarization modulated infrared reflection absorption spectroscopy (PM-IRRAS). Detection limits of 0.128 nmol L^{-1} (electrochemical impedance spectroscopy) and 1.42 nmol L^{-1} (electrical impedance spectroscopy) were reported. For further information on electrochemical and impedance-based biosensors we suggest reading this article.[91]

Kim et al. (**Figure 20**) designed and characterized a label-free impedance biosensor using PEDOT/AuNP composites for detecting VEGF-165.[92] PEDOT/AuNP composites were galvanostatically electropolymerized onto 3 types of electrodes including stainless steel free-standing pads, Au SPEs, and Au interdigitated electrodes (IDEs). Thin films of a PEDOT AuNP composites with uniform thickness were deposited on Au IDEs whereas inhomogeneous layers with the potential to delaminate were reported on gold SPEs and stainless-steel electrodes, resulting in lower reproducibility amongst biosensors. Nyquist plots obtained from the use of IDEs showed a significant change in R_{ct} due to anti-VEGF immobilization and its specific binding to VEGF. For a biosensor with IDEs, R_{ct} was found to have a linear relationship with VEGF over a concentration range of 1–20 pg mL^{-1} and a detection limit of 0.5 pg mL^{-1} was achieved.

Aydın et al. (**Figure 21**) reported a novel and ultrasensitive impedimetric biosensor fabricated using conjugated di-succinimide substituted polythiophene (P(ThidiSuc)) polymer modified indium tin oxide electrode to detect the PSMA.[93] Studies have shown that PSMA is expressed in all types of prostate tissue and that expression is increased in cancerous tissues.[93] The synthesized polymer (P(ThidiSuc)) contains di-succinimide groups, which offered covalent immobilization of PSMA specific antibodies and did not require any cross-linking agent. Under optimum conditions, a wide linear range (0.015 to14.4 pg mL^{-1}), and an LOD of 6.4 fg mL^{-1} were achieved.

PCA3, VEGF, PSMA are not considered to be the best biomarkers so using them as a single biomarker in biosensing seems not a popular approach. However, they are used as complementary biomarkers for dual-mode biosensors. Single biomarker biosensors are commonly associated with false positive results, so the
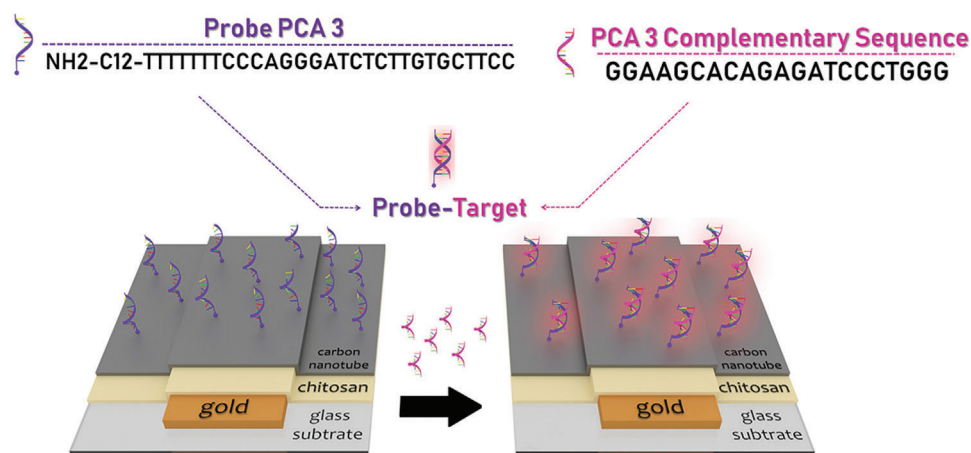

Figure 19. Scheme for the fabrication of a PCA3 biosensor, also showing the pairing owing to hybridization in detecting positive controls. Reproduced with permission.[91] Copyright 2019, American Chemical Society.
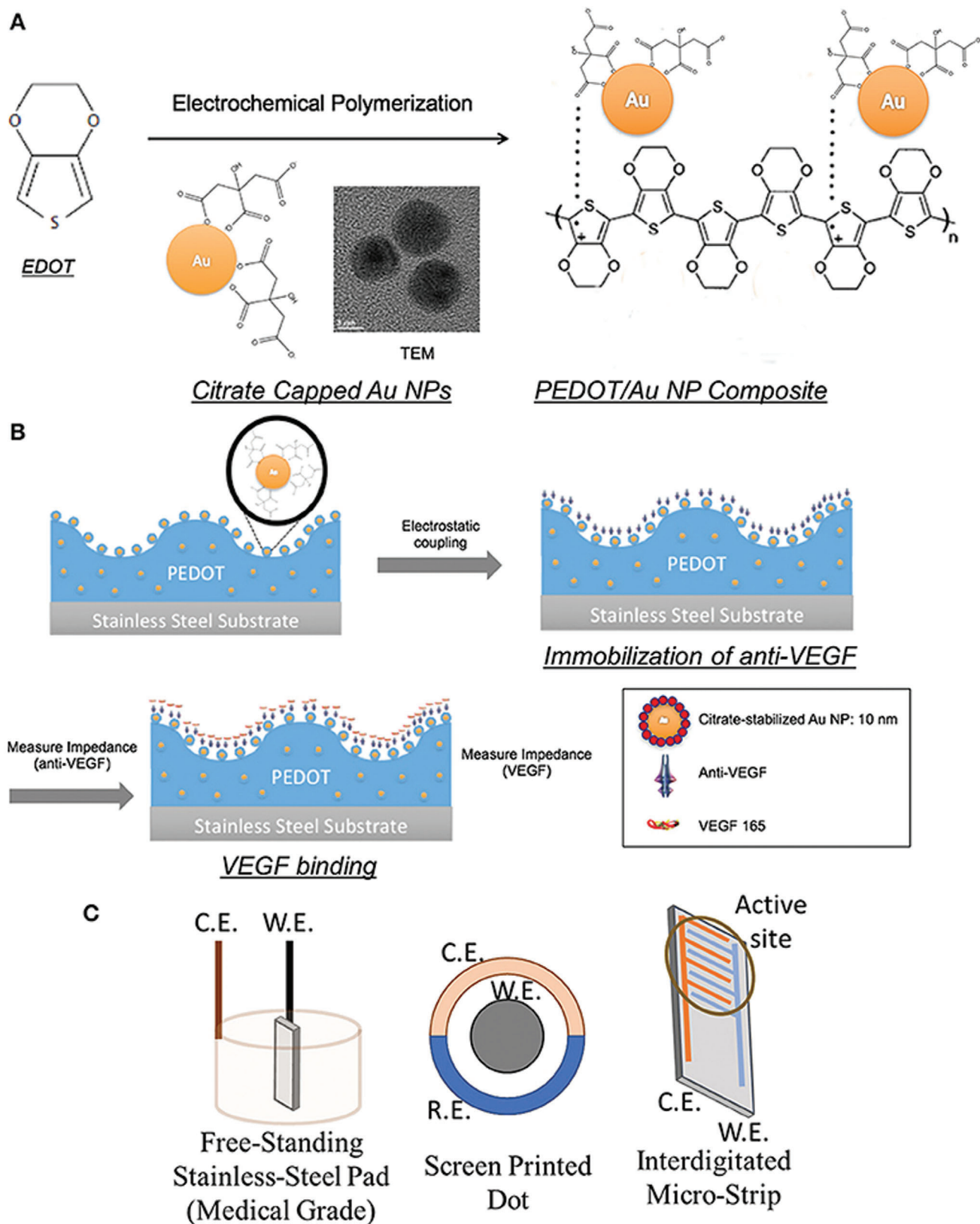
**ADVANCED
SCIENCE NEWS**

www.advancedsciencenews.com

**ADVANCED
MATERIALS
TECHNOLOGIES**

www.advmattechnol.de

Figure 20. Schematics of PEDOT/AuNP composites for VEGF sensors: A) Electrochemical polymerization of PEDOT/Au NP composites. B) Anti-VEGF immobilization and VEGF binding. C) Configurations of working (W.E.), counter (C.E.), and reference (R.E.) electrodes. Reproduced under the terms of the CC-BY license.[92] Copyright 2019, The Authors, published by Frontiers Media.
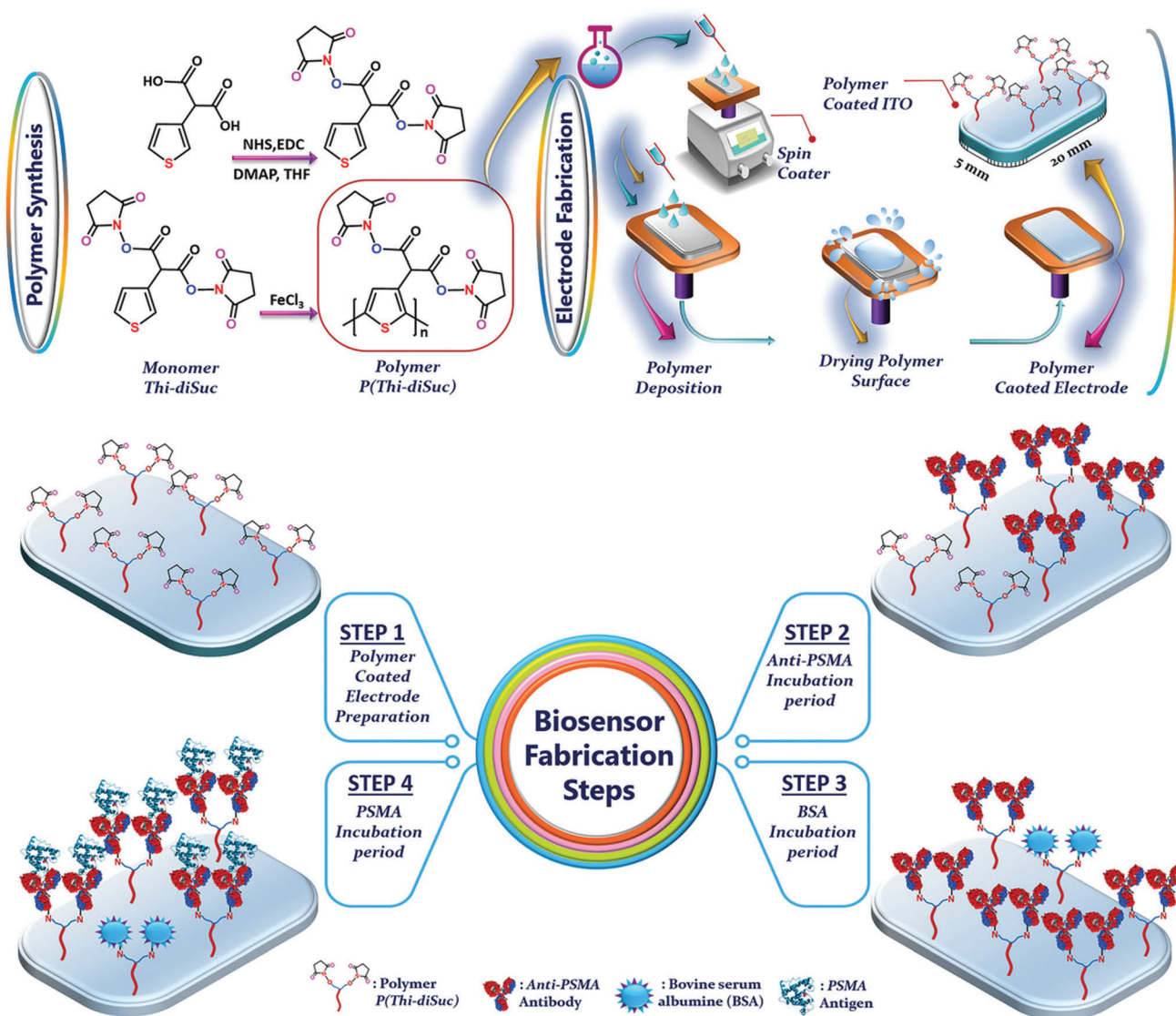
Figure 21. Schematic for polymerP (Thi-diSuc) synthesis and step-by-step fabrication of the biosensor. Reproduced with permission.[93] Copyright 2021, Wiley-VCH.

composition of two different biomarkers into a dual-detection biosensor has become a new development strategy. Back in 2017, Pan et al. created a dual-mode biosensor that can simultaneously detect VEGF and PSA in human serum for the early diagnosis of prostate cancer.[15] They wrapped GO-ssDNA on Au electrode for VEGF detection and combined it with poly(l-propyleneglycolate) nanoparticles (PLLA NPs) for signal amplification and PSA detection (**Figure 22**). It had the advantage of being highly selective, i.e., resistant to interference from external irrelevant proteins. The results showed that the detection limits for VEGF and PSA were 50 pg mL^{-1} and 1 ng mL^{-1}, respectively. M. Sharafeldin et al. assembled Fe$_3$O$_4$ nanoparticles together with an antibody onto GO sheets to produce a multi-functional nanocomposite (**Figure 23**).[94] When the GO-antibody-Fe$_3$O$_4$ nanocomposite specifically combined to PSA and PSMA proteins, the resulting complex could be isolated in a magnetic field and de-

livered in microfluidic channel to an electrochemical detection cell. The Fe$_3$O$_4$–GO particles subsequently catalyze H$_2$O$_2$ reduction, generating a current signal. LOD of 15 fg mL^{-1} of PSA and 4.8 fg mL^{-1} of PSMA were achieved, which were 1000-times better than previously reported PSA biosensors using Fe$_3$O$_4$ only, probably because GO carried more Fe$_3$O$_4$ nanoparticles and thus dramatically increased the electrochemical signal.

In 2021, Sánchez-Salcedo et al. successfully constructed a dual-mode biosensor platform by immobilizing mRNA fragments of PCA3 and PSA on Au electrodes (**Figure 24**).[95] The LOD of PCA3 and PSA reached 4.4 and 1.5 pM, respectively and benefited from the incorporation of multiple redox enzymes to improve sensitivity. Although this is the first electrochemical dual-mode biosensor for the detection of PCA3, it cannot be ignored that the structural stability of mRNA and stable gene expression remains a challenge. The development of a
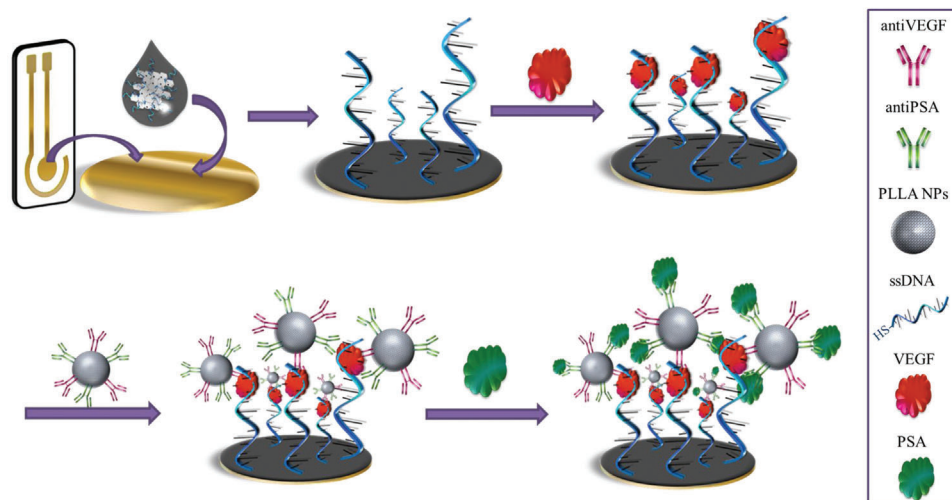
Figure 22. Scheme of electrochemical detection of VEGF and PSA in samples using the GO-ssDNA based biosensor. Reproduced with permission.[15] Copyright 2017, Elsevier.
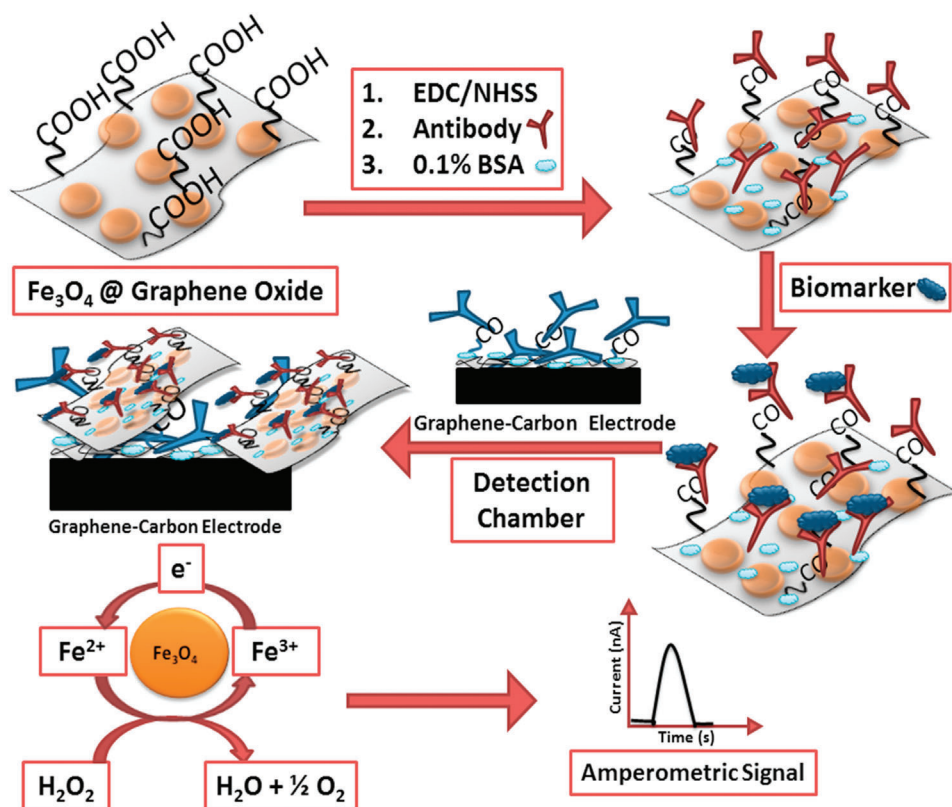

Figure 23. Protein capture and detection mediated by Fe_3O_4@GO sheets. Proteins captured by Fe_3O_4@GO decorated with detection antibodies. Composite with biomarker then captured on the sensor surfaces coated with graphene and capture antibodies. Amperometric signal generated by injecting 100 µL 5 mM H_2O_2. Reproduced with permission.[94] Copyright 2017, Elsevier.

dual-mode biosensor for simultaneous detection of PSA and sarcosine is reported by R. Yan et al. (**Figure 25**).[96] They achieved optimization of PSA and sarcosine sensing systems using hierarchical MoS_2 nanostructures and SiO_2 nanosignal amplification with the LOD of 2.5 and 14.4 fg mL^{-1}, respectively. This is an exciting finding as this method makes it is possible

to directly distinguish cancer patients from healthy patients in clinical serum samples.[96] It is shown that, on the one hand, hierarchical flower-like MoS_2 nanostructures can significantly enhance interfacial accessibility and improve DNA hybridization efficiency. On the other hand, the spherical SiO_2 nanoprobes combined with many electroactive markers and DNA probes can
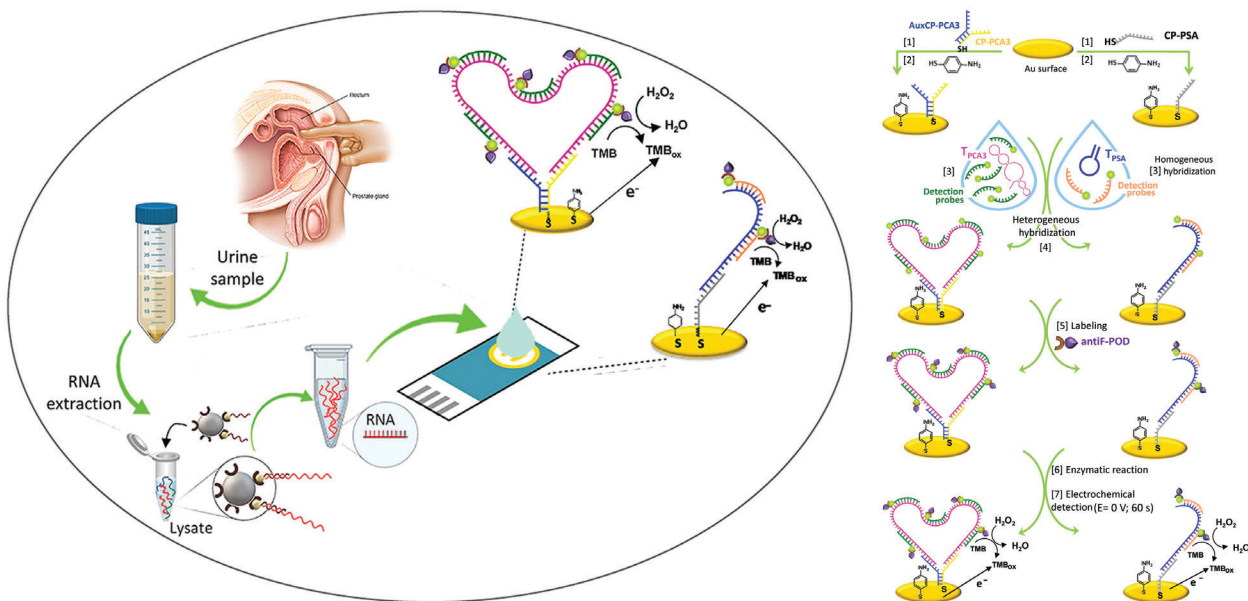
**ADVANCED
SCIENCE NEWS**

www.advancedsciencenews.com

**ADVANCED
MATERIALS
TECHNOLOGIES**

www.advmattechnol.de

Figure 24. Left: Dual electrochemical genosensor for early diagnosis of prostate cancer through lncRNAs detection. **Right**: Steps involved in the construction and operation with the electrochemical genosensor for PCA3 (left) or PSA (right): 1) chemisorption of the thiolated capture structure; 2) blocking with p-aminothiophenol; 3) homogeneous hybridization between the target and the fluorescein-tagged detection probes; 4) heterogeneous hybridization; 5) enzymatic labeling with antiF-POD conjugate; 6) enzymatic reaction; 7) chronoamperometric detection. Reproduced with permission.[95] Copyright 2021, Elsevier.
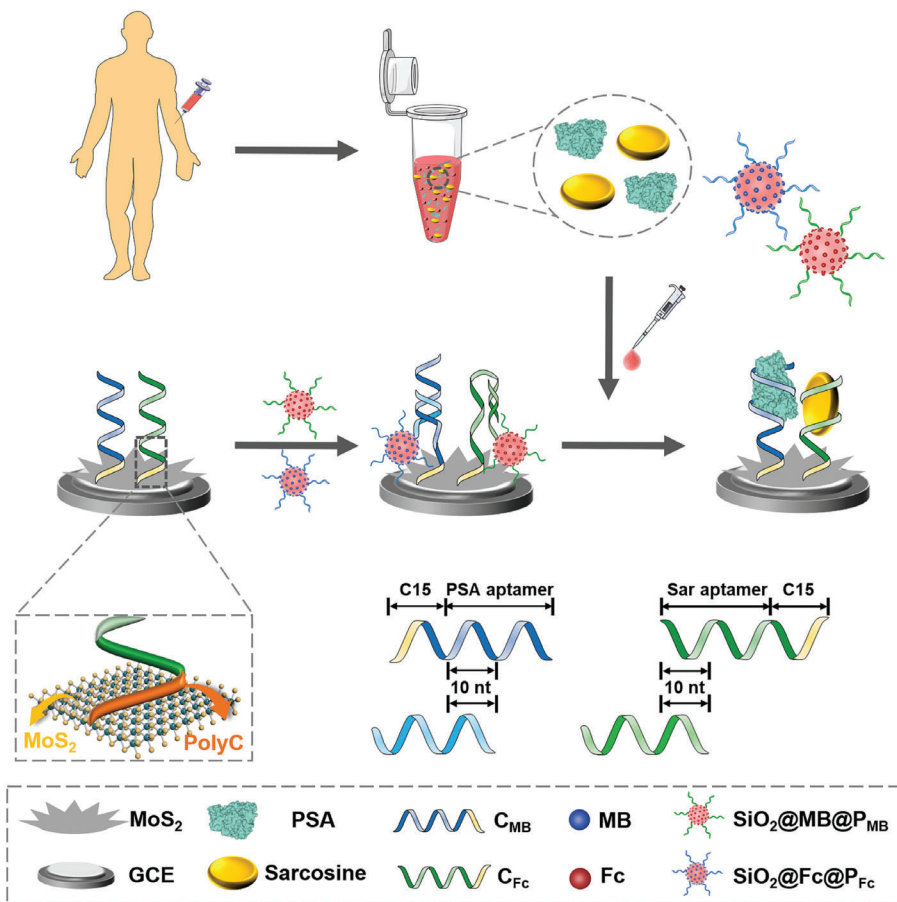

Figure 25. Schematic illustration of electrochemical aptasensor for single-step, simultaneous detection of two tumor markers based on nanoflower-like MoS₂ functional interface and signal amplified SiO₂ nanoprobe.[96] Reproduced with permission.[96] Copyright 2022, Elsevier.

effectively amplify the electrochemical signals. The combination of the two nanomaterials effectively solves the problems of long response time and low signal intensity of the dual-mode biosensor. Most importantly, the successful coupling of two highly plausible PSA biomarkers signifies that this simple, low-cost, pioneering electrochemical sensor will provide a reliable tool for the accurate diagnosis and early detection of prostate cancer.

5. Conclusion and Future Prospects

Although biosensors have been developed for cancer detection, the development of prostate cancer-based biosensors is still progressing slowly. In this review we looked at recent biosensor research for prostate cancer detection with a particular focus on biomarkers and how the incorporation of various nanomaterials has improved biosensor analytical performance. PSA-targeted biosensors (immunosensors, aptamer-based, peptide-based, and nanopore-based biosensors), sarcosine oxidase-targeted biosensors, and other biomarkers-based biosensors (PCA3, VEGF and PSMA) including dual-biomarkers biosensors (PSA-VEGF, PSA-PSMA, PSA-PCA3, PSA-sarcosine) are reviewed and summarized. Modifying the electrodes with noble metals, such as gold, silver, and copper, can undoubtedly improve the signal conduction efficiency, but efficient utilization and economic feasibility needs to be considered. Attaching metal electrode materials to a framework composed of carbon derivatives such as graphene, CNTs not only increases the surface area for specific recognition but also improves the stability of signal transmission. For SO_x biosensors, the application of nanomaterials is mainly focused on the modification of electrodes, where the most used nanomaterials are complexes of graphene, CNTs etc. MXene family nanomaterials such as Ti_3C_2TX, Ti_3AlC_2, etc. are also promising to be important electrode frameworks for redox reactions. In addition, Fe_3O_4, SiO_2, and MoS_2 are also gaining more and more popularity due to their excellent physical properties. Dual-mode biosensors seem have advantages in terms of reliability, thus the development of nanomaterials that are compatible with two or more biomarkers should be a major trend in the future. Also, there are more studies on biomarker detection based in urine and serum, but fewer studies reported in other body fluids (e.g., saliva, seminal fluid). To improve the accuracy and practicality of diagnosis, more studies are expected to perform biomarker detection in various bodily fluids.

Nanomaterials have been employed for innovative biosensor development due to their distinct physical properties resulting from their nanoscale size. Most biosensors for prostate cancer detection are at the proof-of-concept stage and should be rigorously tested and validated for clinical applications. Electrochemical biosensors, being rapid and cost effective, show the potential of integration into portable POC type devices. Their clinical use should be considered during the design stage of nanoparticles/nanomaterials and biosensors, including the biocompatibility, stability, and large-scale production aspects. Multiple detection where researchers can detect several/multiple biomarkers simultaneously should become a future trend. Finally, the development of nanotechnology-based biosensors for prostate cancer detection is a highly interdisciplinary area that will require a robust multidisciplinary approach. Collaboration between clinicians and materials and biosensors experts is essential for successful development and commercialization.

Conflict of Interest

The authors declare no conflict of interest.

[1] F. Bray, M. Laversanne, E. Weiderpass, I. Soerjomataram, *Cancer* **2021**, *127*, 3029.

[2] WHO, URL: https://www.who.int/data/gho/data/themes/mortality-and-global-health-estimates/ghe-leading-causes-of-death **2020**.

[3] W. International, https://www.wcrf.org/cancer-trends/prostate-cancer-statistics/.

[4] S. Singh, A. A. Gill, M. Nlooto, R. Karpoormath, *Biosens. Bioelectron.* **2019**, *137*, 213.

[5] M. Negahdary, N. Sattarahmady, H. Heli, *Clin. Chim. Acta* **2020**, *504*, 43.

[6] a) G. Perry, F. Cortezon-Tamarit, S. I. Pascu, *Front Chem Sci Eng* **2020**, *14*, 4; b) M. J. Barry, *N. Engl. J. Med.* **2001**, *344*, 1373.

[7] V. Naresh, N. Lee, *Sensors* **2021**, *21*, 1109.

[8] P. R. Coulet, L. J. Blum, *Biosensor Principles and Applications*, 1st ed., CRC Press, **1991**. 10.1201/9780367810849.

[9] W. Zhou, P.-J. J. Huang, J. Ding, J. Liu, *Analyst* **2014**, *139*, 2627.

[10] Q. Liu, J. Wang, B. J. Boyd, *Talanta* **2015**, *136*, 114.

[11] a) B. D. Malhotra, M. A. Ali, *Nanomaterials for biosensors: fundamentals and applications*, 1st edition, ISBN: 978-0-323-44923-6 **2018**; b) M. Holzinger, A. Le Goff, S. Cosnier, *Front Chem* **2014**, *2*, 63.

[12] T. Mavrič, M. Benčina, R. Imani, I. Junkar, M. Valant, V. Kralj-Iglič, A. Iglič, *Adv. Biomem. Lip. Self-Assem.* **2018**, *27*, 63.

[13] a) N. Bhalla, Y. Pan, Z. Yang, A. F. Payam, *ACS Nano* **2020**, *14*, 7783; b) F. Huang, Y. Zhang, J. Lin, Y. Liu, *Biosensors* **2021**, *11*, 190.

[14] a) J. R. Prensner, M. A. Rubin, J. T. Wei, A. M. Chinnaiyan, *Sci. Transl. Med.* **2012**, *4*, 127rv3; b) B. Bickers, C. Aukim-Hastie, *Anticancer Res.* **2009**, *29*, 3289; c) V. Kulasingam, E. P. Diamandis, *Nat Clin Pract Oncol* **2008**, *5*, 588.

[15] L.-H. Pan, S.-H. Kuo, T.-Y. Lin, C.-W. Lin, P.-Y. Fang, H.-W. Yang, *Biosens. Bioelectron.* **2017**, *89*, 598.

[16] Y. Wu, R. D. Tilley, J. J. Gooding, *J. Am. Chem. Soc.* **2018**, *141*, 1162.

[17] S. Dowlatshahi, M. J. Abdekhodaie, *Clin. Chim. Acta* **2021**, *516*, 111.

[18] H. Lilja, D. Ulmert, A. J. Vickers, *Nat. Rev. Cancer* **2008**, *8*, 268.

**ADVANCED
SCIENCE NEWS**

www.advancedsciencenews.com

**ADVANCED
MATERIALS
TECHNOLOGIES**

www.advmattechnol.de

[19] M. A. Najeeb, Z. Ahmad, R. Shakoor, A. Mohamed, R. Kahraman, *Talanta* **2017**, *168*, 52.

[20] S. Lara, A. Perez-Potti, *Biosensors* **2018**, *8*, 104.

[21] M. Pal, R. Khan, *Anal. Biochem.* **2017**, *536*, 51.

[22] L. Farzin, S. Sadjadi, M. Shamsipur, S. Sheibani, *J. Pharm. Biomed. Anal.* **2019**, *172*, 259.

[23] a) H. V. Tran, B. Piro, *Microchim. Acta* **2021**, *188*, 128; b) H. Ehtesabi, *Mater. Today Chem.* **2020**, *17*, 100342; c) T. Pasinszki, M. Krebsz, T. T. Tung, D. Losic, *Sensors* **2017**, *17*, 1919; d) D. Damborska, T. Bertok, E. Dosekova, A. Holazova, L. Lorencova, P. Kasak, J. Tkac, *Microchim. Acta* **2017**, *184*, 3049.

[24] J. Feng, Y. Li, M. Li, F. Li, J. Han, Y. Dong, Z. Chen, P. Wang, H. Liu, Q. Wei, *Biosens. Bioelectron.* **2017**, *91*, 441.

[25] M. Khan, K. Dighe, Z. Wang, I. Srivastava, E. Daza, A. Schwartz-Dual, J. Ghannam, S. Misra, D. Pan, *Analyst* **2018**, *143*, 1094.

[26] M. Li, P. Wang, F. Li, Q. Chu, Y. Li, Y. Dong, *Biosens. Bioelectron.* **2017**, *87*, 752.

[27] L. Suresh, P. K. Brahman, K. R. Reddy, J. Bondili, *Enzyme Microb. Technol.* **2018**, *112*, 43.

[28] H. Jia, J. Xu, L. Lu, L. Yu, Y. Zuo, Q. Tian, P. Li, *Sens. Actuators, B* **2018**, *260*, 990.

[29] M. S. Khan, W. Zhu, A. Ali, S. M. Ahmad, X. Li, L. Yang, Y. Wang, H. Wang, Q. Wei, *Anal. Biochem.* **2019**, *566*, 50.

[30] Y. Chen, P.-X. Yuan, A.-J. Wang, X. Luo, Y. Xue, L. Zhang, J.-J. Feng, *Biosens. Bioelectron.* **2019**, *126*, 187.

[31] M. Kukkar, S. K. Tuteja, P. Kumar, K.-H. Kim, A. S. Bhadwal, A. Deep, *Anal. Biochem.* **2018**, *555*, 1.

[32] S. Barman, M. Hossain, H. Yoon, J. Y. Park, *Biosens. Bioelectron.* **2018**, *100*, 16.

[33] F. Li, Y. Li, J. Feng, Y. Dong, P. Wang, L. Chen, Z. Chen, H. Liu, Q. Wei, *Biosens. Bioelectron.* **2017**, *87*, 630.

[34] M. Mahani, F. Alimohamadi, M. Torkzadeh-Mahani, Z. Hassani, F. Khakbaz, F. Divsar, M. Yoosefian, *J. Mol. Liq.* **2021**, *324*, 114736.

[35] H.-M. Kim, M. Uh, D. H. Jeong, H.-Y. Lee, J.-H. Park, S.-K. Lee, *Sens. Actuators, B* **2019**, *280*, 183.

[36] S. Larson, Z. Yang, Y. Zhao, *Chem. Commun.* **2019**, *55*, 1342.

[37] J. Jatschka, A. Dathe, A. Csáki, W. Fritzsche, O. Stranik, *Sens Biosensing Res* **2016**, *7*, 62.

[38] a) A. Azzouz, L. Hejji, K.-H. Kim, D. Kukkar, B. Souhail, N. Bhardwaj, R. J. Brown, W. Zhang, *Biosens. Bioelectron.* **2022**, *197*, 113767; b) Z. Fattahi, A. Y. Khosroushahi, M. Hasanzadeh, *Biomed. Pharmacother.* **2020**, *132*, 110850.

[39] H.-M. Kim, D. H. Jeong, H.-Y. Lee, J.-H. Park, S.-K. Lee, *Opt. Laser Technol.* **2019**, *114*, 171.

[40] H.-M. Kim, J.-H. Park, D. H. Jeong, H.-Y. Lee, S.-K. Lee, *Sens. Actuators, B* **2018**, *273*, 891.

[41] H.-M. Kim, J.-H. Park, S.-K. Lee, *Sci. Rep.* **2019**, *9*, 15605.

[42] D. M. Rissin, C. W. Kan, T. G. Campbell, S. C. Howes, D. R. Fournier, L. Song, T. Piech, P. P. Patel, L. Chang, A. J. Rivnak, *Nat. Biotechnol.* **2010**, *28*, 595.

[43] E. Campos-Fernández, N. O. Alqualo, L. C. M. Garcia, C. C. H. Alves, T. D. F. A. Vieira, D. C. Moreira, V. Alonso-Goulart, *Clin. Biochem.* **2021**, *93*, 9.

[44] S. M. Shaban, D.-H. Kim, *Sensors* **2021**, *21*, 979.

[45] P. Jolly, P. Zhurauski, J. L. Hammond, A. Miodek, S. Liébana, T. Bertok, J. Tkáč, P. Estrela, *Sens. Actuators, B* **2017**, *251*, 637.

[46] S. Hassani, A. S. Maghsoudi, M. R. Akmal, S. R. Rahmani, P. Sarihi, M. R. Ganjali, P. Norouzi, M. Abdollahi, *J. Pharm. Pharm. Sci.* **2020**, *23*, 243.

[47] L. He, R. Huang, P. Xiao, Y. Liu, L. Jin, H. Liu, S. Li, Y. Deng, Z. Chen, Z. Li, *Chin. Chem. Lett.* **2021**, *32*, 1593.

[48] B. Wei, K. Mao, N. Liu, M. Zhang, Z. Yang, *Biosens. Bioelectron.* **2018**, *121*, 41.

[49] S. S. Sekhon, P. Kaur, Y.-H. Kim, S. S. Sekhon, *npj 2D Mater. Appl.* **2021**, *5*, 21.

[50] S. S. Shahbazi Toloun, L. Pishkar, *Mol. Simul.* **2021**, *47*, 951.

[51] Y. Khan, A. Li, L. Chang, L. Li, L. Guo, *Sens. Actuators, B* **2018**, *255*, 1298.

[52] F. Duan, S. Zhang, L. Yang, Z. Zhang, L. He, M. Wang, *Anal. Chim. Acta* **2018**, *1036*, 121.

[53] a) B. Huang, X.-P. Liu, J.-S. Chen, C.-j. Mao, H.-L. Niu, B.-K. Jin, *Microchim. Acta* **2020**, *187*, 155; b) X. Zhou, L. Yang, X. Tan, G. Zhao, X. Xie, G. Du, *Biosens. Bioelectron.* **2018**, *112*, 31.

[54] X.-P. Liu, N. Chang, J.-S. Chen, C.-J. Mao, B.-K. Jin, *Microchem. J.* **2021**, *168*, 106337.

[55] H. Park, G. Han, S. W. Lee, H. Lee, S. H. Jeong, M. Naqi, A. AlMutairi, Y. J. Kim, J. Lee, W.-j. Kim, *ACS Appl. Mater. Interfaces* **2017**, *9*, 43490.

[56] M. Wang, L. Li, L. Zhang, J. Zhao, Z. Jiang, W. Wang, *Anal. Chem.* **2021**, *94*, 431.

[57] L. Yuan, L. Liu, *Sens. Actuators, B* **2021**, *344*, 130232.

[58] P. S. Sfragano, G. Moro, F. Polo, I. Palchetti, *Biosensors* **2021**, *11*, 246.

[59] F. Meng, H. Sun, Y. Huang, Y. Tang, Q. Chen, P. Miao, *Anal. Chim. Acta* **2019**, *1047*, 45.

[60] C. Ding, X. Wang, X. Luo, *Anal. Chem.* **2019**, *91*, 15846.

[61] S. Joshi, P. Sharma, R. Siddiqui, K. Kaushal, S. Sharma, G. Verma, A. Saini, *Microchim. Acta* **2020**, *187*, 27.

[62] J. Yoon, J. Lim, M. Shin, S.-N. Lee, J.-W. Choi, *Materials* **2021**, *14*, 518.

[63] Z. Ye, G. Li, X. Xu, Q. Yu, X. Yue, Y. Wu, B. Ye, *Talanta* **2020**, *209*, 120611.

[64] a) S. Meng, Y. Zhang, H. Wang, L. Wang, T. Kong, H. Zhang, S. Meng, *Biomaterials* **2021**, *269*, 120471; b) L. Ding, Y. Chang, P. Yang, W. Gao, M. Sun, Y. Bie, L. Yang, X. Ma, Y. Guo, *Mater. Sci. Eng., C* **2020**, *117*, 111371; c) S. Shukla, P. Arora, *Optik* **2021**, *228*, 166196.

[65] Y. Xu, X. Wang, C. Ding, X. Luo, *ACS Appl. Mater. Interfaces* **2021**, *13*, 20388.

[66] N. Hui, J. Wang, D. Wang, P. Wang, X. Luo, S. Lv, *Biosens. Bioelectron.* **2022**, *200*, 113921.

[67] J. H. Choi, H. S. Kim, J.-W. Choi, J. W. Hong, Y.-K. Kim, B.-K. Oh, *Biosens. Bioelectron.* **2013**, *49*, 415.

[68] N. Xia, D. Deng, S. Yang, Y. Hao, L. Wang, Y. Liu, C. An, Q. Han, L. Liu, *Sens. Actuators, B* **2019**, *291*, 113.

[69] S. Xie, J. Zhang, Y. Yuan, Y. Chai, R. Yuan, *Chem. Commun.* **2015**, *51*, 3387.

[70] D. Wang, Y. Zheng, Y. Chai, Y. Yuan, R. Yuan, *Chem. Commun.* **2015**, *51*, 10521.

[71] Y. He, S. Xie, X. Yang, R. Yuan, Y. Chai, *ACS Appl. Mater. Interfaces* **2015**, *7*, 13360.

[72] H. Qi, M. Li, M. Dong, S. Ruan, Q. Gao, C. Zhang, *Anal. Chem.* **2014**, *86*, 1372.

[73] L. Yang, N. Li, K. Wang, X. Hai, J. Liu, F. Dang, *Talanta* **2018**, *179*, 531.

[74] J. Zhao, S. Wang, S. Zhang, P. Zhao, J. Wang, M. Yan, S. Ge, J. Yu, *Biosens. Bioelectron.* **2020**, *150*, 111958.

[75] K. Chuah, Y. Wu, S. Vivekchand, K. Gaus, P. J. Reece, A. P. Micolich, J. J. Gooding, *Nat. Commun.* **2019**, *10*, 2109.

[76] Y. Wu, Y. Yao, S. Cheong, R. D. Tilley, J. J. Gooding, *Chem. Sci.* **2020**, *11*, 12570.

[77] Y. Lin, Y.-L. Ying, X. Shi, S.-C. Liu, Y.-T. Long, *Chem. Commun.* **2017**, *53*, 11564.

[78] V. Narwal, P. Kumar, P. Joon, C. Pundir, *Enzyme Microb. Technol.* **2018**, *113*, 44.

[79] P. Kumar, V. Narwal, R. Jaiwal, C. Pundir, *Biosens. Bioelectron.* **2018**, *122*, 140.

[80] R. Deswal, V. Narwal, P. Kumar, V. Verma, A. S. Dang, C. Pundir, *Sensors International* **2022**, *3*, 100174.

[81] D. Uhlirova, M. Stankova, M. Docekalova, B. Hosnedlova, M. Kepinska, B. Ruttkay-Nedecky, J. Ruzicka, C. Fernandez, H. Milnerowicz, R. Kizek, *Int. J. Mol. Sci.* **2018**, *19*, 3722.

[82] S. Hroncekova, T. Bertok, M. Hires, E. Jane, L. Lorencova, A. Vikartovska, A. Tanvir, P. Kasak, J. Tkac, *Processes* **2020**, *8*, 580.

[83] Q. Yang, N. Li, Q. Li, S. Chen, H.-L. Wang, H. Yang, *Anal. Chim. Acta* **2019**, *1078*, 161.

[84] T. S. Rebelo, C. M. Pereira, M. G. F. Sales, J. P. Noronha, J. Costa-Rodrigues, F. Silva, M. H. Fernandes, *Anal. Chim. Acta* **2014**, *850*, 26.

[85] T. Rajarathinam, M. Kwon, D. Thirumalai, S. Kim, S. Lee, J.-H. Yoon, H.-j. Paik, S. Kim, J. Lee, H. K. Ha, *Anal. Chim. Acta* **2021**, *1175*, 338749.

[86] X. Zhang, J. Chen, Q. Wang, B. Du, G. Fan, W. Zheng, H. Yang, T. Xu, *Electroanalysis* **2022**, *34*, 345.

[87] Y. Zhou, H. Yin, X. Meng, Z. Xu, Y. Fu, S. Ai, *Electrochim. Acta* **2012**, *71*, 294.

[88] H. Yang, J. Wang, C. Yang, X. Zhao, S. Xie, Z. Ge, *J. Electrochem. Soc.* **2018**, *165*, H247.

[89] Q. Wang, C. Yang, Q. Yang, S. Yu, H. Yang, *Anal. Chim. Acta* **2019**, *1046*, 93.

[90] J. Feng, X. Chen, X. Shi, W. Zheng, X. Zhang, H. Yang, *ECS J. Solid State Sci. Technol.* **2022**, *11*, 047001.

[91] J. C. Soares, A. C. Soares, V. C. Rodrigues, M. E. Melendez, A. C. Santos, E. F. Faria, R. M. Reis, A. L. Carvalho, O. N. Oliveira Jr, *ACS Appl. Mater. Interfaces* **2019**, *11*, 46645.

[92] M. Kim, R. Iezzi Jr, B. S. Shim, D. C. Martin, *Front Chem* **2019**, *7*, 234.

[93] E. B. Aydın, M. Aydın, M. K. Sezgintürk, *Macromol. Biosci.* **2021**, *21*, 2100173.

[94] M. Sharafeldin, G. W. Bishop, S. Bhakta, A. El-Sawy, S. L. Suib, J. F. Rusling, *Biosens. Bioelectron.* **2017**, *91*, 359.

[95] R. Sánchez-Salcedo, R. Miranda-Castro, N. de-Los-Santos-Álvarez, M. J. Lobo-Castañón, *Biosens. Bioelectron.* **2021**, *192*, 113520.

[96] R. Yan, N. Lu, S. Han, Z. Lu, Y. Xiao, Z. Zhao, M. Zhang, *Biosens. Bioelectron.* **2022**, *197*, 113797.

Baljit Singh is a Principal Investigator and Senior-Business-Development-Professional (TU Dublin), contributing to applied research, business-development/management, and commercialization activities. Dr Singh contributed immensely to the establishment of Enterprise-Ireland Technology Gateway 'MiCRA Biodiagnostics' and worked with a range of start-ups/SMEs and multinational companies. He delivered several collaborative industry-research-projects and is a key contributor to the innovation-technologies developed at MiCRA Biodiagnostics. He received M.Tech (Advanced-Chemical-Analysis, IIT-Roorkee, India), PhD (Electroanalytical Chemistry/Sensors-Nanomaterials, TU Dublin) followed by Postdoctoral, Senior-Postdoctoral-Research-Fellow and Business-Development positions. Dr Singh also worked as a Lecturer & Associate Lecturer (Chemistry, TU Dublin) and Lecturer (Chemistry, D.A.V. College Pehowa, India). Dr Singh is a Guest Editor: Bioelectrochemistry (ELSEVIER), Biosensors (MDPI), Chemosensors (MDPI) and Associate Editor (Nanomaterials, Frontiers in Nanotechnology). He reviewed a number of articles for RSC/ACS/Elsevier/MDPI journals. **Research interests**: Electrochemical sensors/biosensors for human & animal diagnostics, agri-food/dairy and environmental analysis, biomarkers & point-of-care devices, nanomaterials, design-engineering of electrode-detection & microfluidic-reagent systems.

Shiliang Ma is working with a Chinese pharmaceutical Industry. Shiliang received his Bachelor of Pharmacy degree from Shanghai University in Traditional Chinese Medicine in 2019. He graduated (Master's degree in Biotherapeutics) from University College Dublin (UCD), Dublin, Ireland in 2022. He also worked on a research project under the supervision of Dr. Baljit Singh at TU Dublin. **Research interests**: Biosensors, screen printed electrodes, nanomaterials, immunoassay, and pharmaceutical analysis.

**ADVANCED
SCIENCE NEWS**

www.advancedsciencenews.com

**ADVANCED
MATERIALS
TECHNOLOGIES**

www.advmattechnol.de

Tony O Hara works as an Environmental Chemist at the Department of Agriculture, Food & Marine, Ireland. He was previously employed at the State Laboratory Ireland. Prior to this, Tony worked as a Postdoctoral Researcher at the School of Chemical Sciences, Dublin City University where he aided in the development of a prototype electrolyser for green hydrogen generation. Tony completed his PhD in 2016 at the Technological University Dublin. His PhD research involved the development of a whole cell electrochemical biosensor for environmental toxicant screening applications. **Research interests**: Development of electrochemical sensors/biosensors for environmental sensing applications.
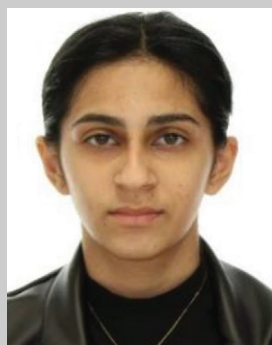
Sargun Singh is a self-motivated explorer/learner and young student (Old Bawn Community School, Dublin 24, Ireland) with strong interest in scientific innovations in protecting public health, animals, and our water & environmental resources. Sargun has a good background in Biology and Chemistry. Sargun was the overall winner of Trinity College Dublin (TCD) TY Language Poster Competition 2020 (Medal & Award). She delivered a speech on "Carbon Footprint" in the National Museum of Ireland (Dublin, April 2023) for the Youth-Assembly & RTÉ. She also delivered an awareness speech "Vaisakhi & Environment" at "Vaisakhi Festival 2023" hosted by Punjabi-Radio-Ireland & Irish-Punjabi-Association (Dublin, Ireland) where she received Honour and Award for her contribution.
Research interests: Environmental contaminants/pollutants, carbon footprint, water sustainability, nanomaterials, biosensors, antibiotics/AMR.